ROMANIAN ACADEMY
School of Advanced Studies of the Romanian Academy
Institute of Biology Bucharest

PhD THESIS - SUMMARY

BIOSYNTHESIS OF NOBLE METAL NANOPARTICLES BY MICROORGANISMS, FUNDAMENTAL AND APPLICATIVE ASPECTS

PhD COORDINATOR:
Senior Researcher Dr. Cristina Ligia PURCĂREA

Phd STUDENT:
Adrian GHINEA

2025

TABLE OF CONTENT

INTRODUCTION

In recent decades, nanotechnology has become one of the most promising and dynamic fields of scientific research, generating innovative solutions in biomedicine, industry, electronics, agriculture, and environmental protection. This rise is largely due to the development and application of nanomaterials, among which nanoparticles (NPs) occupy a central position owing to their unique physicochemical properties and functional versatility (Daniel and Astruc, 2004; Jeevanandam et al., 2018; Altammar, 2023).

NPs are typically defined as particles with sizes between 1 and 100 nm, exhibiting properties that differ from those of the bulk material (Potocnik, 2011; Batista et al., 2015). These include a very high specific surface area, size-dependent quantum effects, altered optical and magnetic behavior, and increased chemical reactivity relative to their bulk counterparts (Buzea et al., 2007; Chen et al., 2010; Amendola and Meneghetti, 2013). Such features endow NPs with advanced capabilities to interact with biological molecules, heavy metals, toxic substances, and radiation, opening multiple avenues for application.

NPs can be classified by chemical composition (metallic, non-metallic, hybrid); by the nature of the element or compound (noble, transition, metal oxides); by synthesis method (physical, chemical, biological); and by application domain. Metallic nanoparticles (MNPs) are particularly valuable for biomedical and environmental uses due to their chemical reactivity, stability, and amenability to functionalization with bioactive molecules (Suresh et al., 2011; Dykman and Khlebtsov, 2012). Among these, gold (AuNPs), silver (AgNPs), platinum (PtNPs), and palladium (PdNPs) nanoparticles are especially important for their optical (plasmonic), catalytic, and biological properties.

The properties of MNPs arise from their extremely small dimensions and very large surface area; consequently, they can interact with other substances or with light in ways that differ from metal particles at the macroscale (Chen et al., 2010; Zou et al., 2021).

Conventional nanoparticle synthesis methods—chemical and physical—while efficient and relatively controllable, entail major drawbacks: high costs, generation of toxic by-products, use of organic solvents, and substantial energy requirements (Narayanan and Sakthivel, 2010; Khan et al., 2017). Consequently, there has been a marked shift toward biological synthesis (biosynthesis) as a greener, more sustainable alternative, which employs plants, fungi, algae, or bacteria to reduce metal ions and stabilize nanoparticles (Iravani, 2014; Keat et al., 2015; Kora and Rastogi, 2015). One microbial example is *Shewanella oneidensis* MR-1, a Gram-negative bacterium with versatile metabolism that can reduce a broad range of metal compounds (Beliaev et al., 2001; Pirbadian et al., 2014).

The growing global interest in biosynthesized metallic nanoparticles (MNPs) reflects the need for innovative and sustainable solutions to complex challenges in health care, environmental protection, and advanced technological industries (Alsaba et al., 2020; Rafeeq et al., 2022; Haleem et al., 2023). Against the backdrop of mounting concerns about the environmental and human-health impacts of traditional synthesis routes, biological methods stand out as promising, safe, and eco-friendly alternatives. Biosynthesis of MNPs using microorganisms and biological extracts not only minimizes the use of toxic chemical agents and energy-intensive steps, but also yields products with high biocompatibility, which makes them well suited for biomedical, pharmaceutical, and environmental applications (Li et al., 2017; Peng et al., 2018).

This broad conceptual framework motivates research aimed at elucidating the fundamental biological mechanisms underlying MNP biosynthesis; optimizing experimental conditions and production parameters; and assessing the efficacy, stability, and safety of the resulting nanomaterials under realistic use conditions.

In this context, the present work adopts an integrative, multidimensional approach to the biosynthesis of gold (Au), silver (Ag), platinum (Pt), and palladium (Pd) nanoparticles using the bacterial strain *Shewanella oneidensis* MR-1. The choice of this organism rests on its inherent capacity to reduce metal ions, making it an attractive and relevant biological model for the sustainable production of nanomaterials.

CHAPTER I – STATE OF THE ART

1.1. General classification of metallic nanoparticle (MNP) synthesis methods

The synthesis of metallic nanoparticles (MNPs) is a core area of modern nanotechnology, with direct implications for the development of advanced functional materials for biomedical, catalytic, environmental, and industrial applications. The synthesis route governs not only nanoparticle formation but also size, shape, size distribution, stability, and functionality, which makes method selection a critical step in designing the final material (Iravani, 2011; Jeevanandam et al., 2018).

Conceptually, nanoparticle synthesis can be grouped into two fundamental paradigms: top-down and bottom-up. Top-down approaches fragment bulk materials down to the nanoscale by physical–mechanical or lithographic procedures—mechanical milling (ball milling), electron-beam lithography, laser ablation—offering access to metals that are difficult to obtain chemically and good control over chemical purity, but at the cost of high expenses, specialized equipment, possible abrasive contamination, and, at times, limited control over particle size and shape (Ng et al., 2013; Heim, 2011). By contrast, bottom-up strategies self-assemble atomic or ionic species into nanoparticles via chemical/physical/biological reduction—including redox reactions in solution, vapor-phase processes (deposition, evaporation–condensation), and green syntheses using plants, bacteria, fungi, or enzymes—providing superior control over nucleation, size, and morphology, straightforward surface functionalization, and broad coverage of metals and alloys (Amendola and Meneghetti, 2013; Iravani, 2014). In practice, synthesis methods are commonly organized into three operational classes: physical, chemical, and biological.

1.2. Physical synthesis methods

Physical methods for MNP synthesis are among the oldest and most extensively studied techniques for producing nanomaterials. These approaches apply direct physical forces—such as heat, radiation, pressure, or friction—to fragment bulk materials or to condense metal vapors into nanoscale particles. Generally classified within the top-down paradigm, they enable the production of high-purity nanoparticles without the use of potentially toxic chemical reagents (Jeevanandam et al., 2018; Baig et al., 2021).

1.3. Chemical synthesis methods

Chemical synthesis methods are among the most widely used and thoroughly studied routes for obtaining MNPs, owing to their versatility, scalability, and relatively precise control over particle size and shape. These approaches rely primarily on the reduction of metal ions in solution in the presence of reducing agents and stabilizers that prevent agglomeration and enable colloidal stabilization of the resulting nanoparticles (Iravani, 2011; Jeevanandam et al., 2018). In general, chemical synthesis transforms metal salts (e.g., $AgNO_3$, $HAuCl_4$, H_2 $PtCl_6$, $PdCl_2$) into zero-valent metal atoms (Ag^0 , Au^0 , Pt^0 , Pd^0), which nucleate and then grow by aggregation to form nanoparticles. The process typically involves two essential components: reducing agents, which convert metal ions to the crystalline metallic state, and stabilizing (capping) agents, which bind to the nanoparticle surface and prevent agglomeration or side reactions (Schmidt, 2001; Arulmozhi and Mythili, 2013).

One of the major limitations of chemical synthesis is the toxicity of residual reagents, which can remain on nanoparticle surfaces even after multiple washing steps. These compounds may affect living cells by inducing oxidative stress or inflammation, thereby limiting the direct use of nanoparticles in biomedical applications without additional functionalization (Iravani, 2014; Siddiqi and Husen, 2016).

1.4. Biological synthesis of nanoparticles

Unlike conventional approaches, biological synthesis does not require toxic reducing agents or hazardous organic solvents. It relies on the intrinsic ability of biological systems to reduce metals via bioactive molecules such as enzymes, proteins, flavonoids, terpenoids, amino acids, or redox cofactors (Ahmad et al., 2016; Khan et al., 2017; El-Rafai et al., 2018). The process typically proceeds under mild reaction conditions, which is advantageous for applications in biomedicine, pharmacology, and the food industry.

Bacteria can synthesize nanoparticles either intracellularly—through enzyme-mediated mechanisms in the cytoplasm or cell envelope—or extracellularly, through the secretion of redox-active compounds (He et al., 2007; Iravani, 2011; Ardelean, 2015; Moisescu et al., 2014). Species such as Shewanella oneidensis MR-1 (Burgos et al., 2008), Geobacter sulfurreducens (Yates et al., 2013), Pseudomonas stutzeri (Haefeli et al., 1984; Husseiny et al., 2007), Escherichia coli (Attard et al., 2012), and Stenotrophomonas maltophilia (Nangia et al., 2009) have been documented as efficient at reducing metal salts and forming nanoparticles of Ag, Au, Pd, Pt, and ZnO.

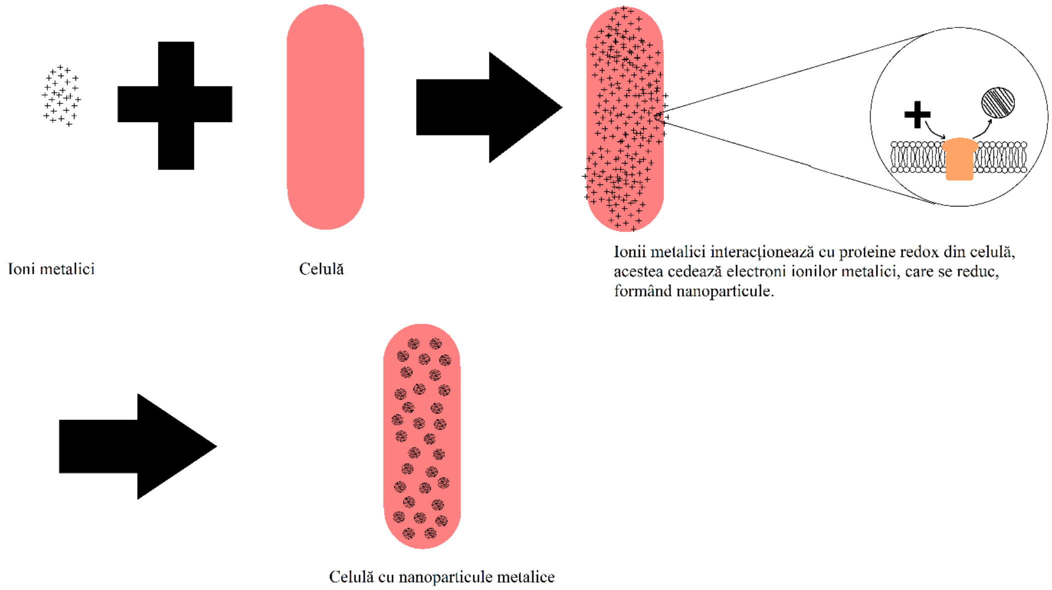

Figure 1. Nanoparticle synthesis mediated by bacterial cells (McMillan et al., 2012).

1.5. Biological mechanisms involved in MNP formation

Biological synthesis of MNPs relies on interactions between metal ions and cellular or extracellular components of living systems, which drive reduction, nucleation, and stabilization at the nanoscale. Common steps are shared by both intracellular and extracellular routes (Iravani, 2011; Ahmad et al., 2016).

First, metal ions are introduced into an active biological system (cells or extracts) and interact with bioactive molecules.

Second, the ions are reduced by endogenous reductants—such as flavins, enzymes, glutathione, or thiol-containing proteins—yielding zero-valent atoms (e.g., $Ag^+ \rightarrow Ag^0$).

Finally, metallic nuclei form and grow into nanoparticles that are stabilized by surface-bound biomolecules (e.g., polysaccharides, peptides, amino acids), which prevent the aggregation of NPs.

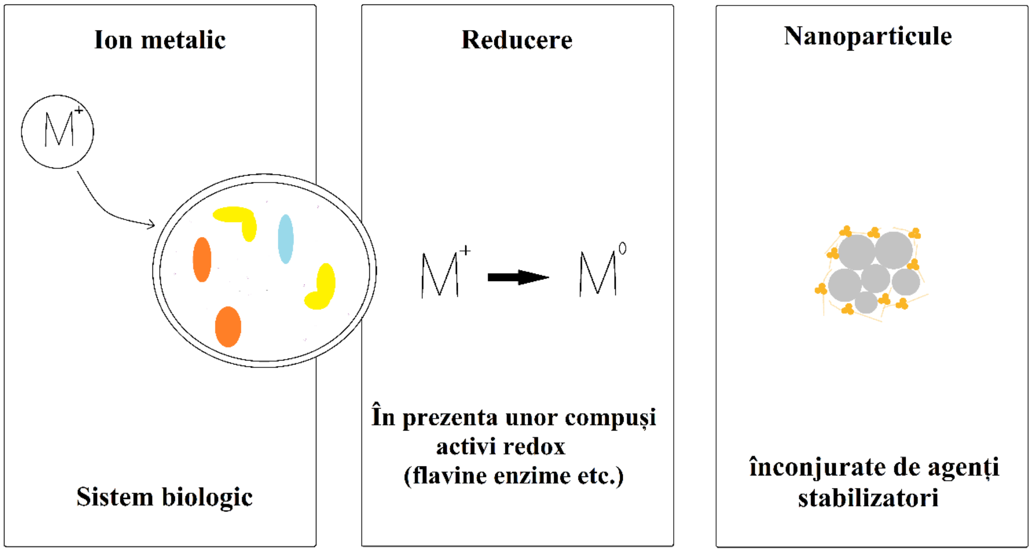

Figure 2. Stages of metallic nanoparticle biosynthesis: (1) adsorption of metal ions onto the cell membrane; (2) reduction of metal ions in the presence of redox-active compounds; (3) formation and stabilization of nanoparticles (Das et al., 2022).

In this work, we focus specifically on the reduction of metal ions via extracellular redox mediators secreted into the medium, as well as on reduction mediated by anaerobic respiration. During anaerobic respiration, electrons (e^-) donated by an oxidizable organic substrate are taken up by the cellular respiratory chain and transferred to a terminal electron acceptor, which may be an organic compound (e.g., fumarate), an oxyanion (e.g., nitrate, sulfate, carbonate), or metal ions; electron transfer along the respiratory chain is coupled to membrane-associated oxidative phosphorylation (Lazăr et al., 2017).

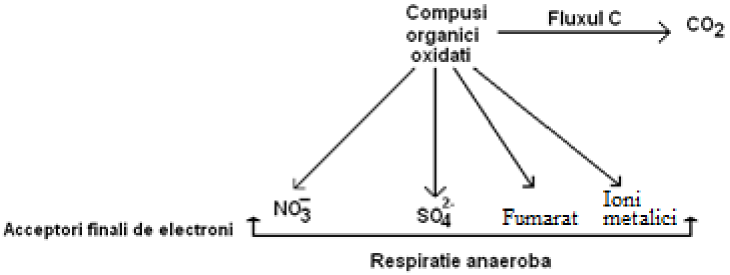

Figure 3. Terminal electron acceptors in anaerobic respiration. Catabolism of organic compounds yields CO_2 (Lazăr et al., 2017).

1.6. Modern and hybrid synthesis techniques

As the field of nanotechnology has advanced, there has been an increasingly pressing need for synthesis routes that combine the advantages of conventional (chemical and physical) strategies with the sustainability and biocompatibility of biological synthesis. Consequently, modern and hybrid methods have been developed in which principles from multiple categories are integrated to obtain MNPs with optimized physicochemical properties and advanced functionality (Eze and Nwabor, 2020). These emerging techniques enable the production of nanoparticles with controlled sizes, enhanced stability, high purity, and strong biocompatibility, while at the same time employing milder experimental conditions and greener processes (Iravani, 2014; Jeevanandam et al., 2018).

1.6.1. Hybrid biochemical systems

An important direction in MNP synthesis is the combination of biological agents with chemical catalysts or physical factors (e.g., temperature, pH, light) to increase reaction rates, tighten size control, and tailor surface functionality. Examples include using plant extracts together with heat or UV irradiation to accelerate synthesis (Zayadi and Bakar, 2020); employing bacteria or fungi in the presence of sub-lethal concentrations of chemical reductants (Narayanan and Sakthivel, 2010); or partial chemical reduction followed by stabilization with biological proteins to obtain nanoparticles with dual (chemical + biological) capping (Ahmad et al., 2016). These methods reduce the amount of chemical reagents while improving nanoparticle uniformity and colloidal stability.

1.6.2. Use of spent culture medium (“spent medium”)

A significant advance in biological MNP synthesis is the use of spent culture medium (supernatant) containing redox-active metabolites secreted by microorganisms (Saif, 2022; Boldt et al., 2023). This strategy constitutes an innovative route to extracellular synthesis. Its benefits include eliminating the need to maintain cell viability, avoiding bacterial contamination of nanoparticles, and enabling automation and industrial scaling (Eze and Nwabor, 2020). A notable example is Shewanella oneidensis MR-1, whose spent medium contains flavins and other redox molecules capable of reducing Ag^+, Au^{3+}, Pd^{2+}, and Pt^{4+} ions to generate stable, biologically active nanoparticles (Marsili et al., 2008; Pirbadian et al., 2014).

1.6.3. Light-assisted synthesis

Certain biological MNP syntheses can be stimulated or accelerated by light exposure, particularly in the presence of photosensitive compounds (flavins, chlorophylls, and polyphenols). This approach involves activating redox-active molecules under white or UV light, generating electrons or reactive oxygen species that reduce metal ions, while controlling nanoparticle shape and size by adjusting illumination intensity and duration (Thatoi et al., 2016; Hunag et al., 2019).

1.7. Considerations on the scalability, cost, and sustainability of MNP synthesis methods

In the context of large-scale applications of nanomaterials, the choice of MNP synthesis method must consider not only scientific efficiency and the quality of the final product, but also industrial scalability, associated costs, and environmental impact. These aspects become critical particularly in sectors such as biomedicine, pharmaceuticals, cosmetics, and environmental remediation, where safety, reliability, and sustainability are essential (Iravani, 2011; Jeevanandam et al., 2018).

Taking into account the costs of equipment, reagents, and operational and purification steps (Singh et al., 2002; Iravani, 2014; Thanh et al., 2014; Hasan, 2015; Balachandran et al., 2022; Hachem et al., 2022), applying physical, chemical, or biological methods to obtain MNPs can result in markedly different total costs (Table 1).

Table 1. Cost analysis of the three categories of nanoparticle synthesis methods.

Method type	Equipment cost	Reagents Cost	Operating cost	Purification cost	Estimated total
Physical	Very high	Low	High	Low	Very high
Chemical	Medium	High	Medium	High	High
Biological	Low	Low	Low	Low	Low-medium

Thus, the reliance on expensive equipment in physical methods leads to very high overall costs, whereas the medium-to-high expenditures at each stage of chemical synthesis result in relatively high total costs—though still lower than those of physical methods (Table 1). By contrast, biological synthesis—particularly when using plant extracts or non-pathogenic bacteria—is associated with reduced costs owing to the use of natural feedstocks, the wide availability of biological reducing agents, and lower energy requirements (Sharma et al., 2012; Veisi et al., 2017).

1.8. Use of bacteria in MNP synthesis

Compared with plants or fungi, bacteria offer key advantages for biosynthesis: shorter reaction times due to rapid life cycles; ease of genetic manipulation, enabling metabolic pathway tuning to optimize synthesis; the ability to grow in diverse environments, including extreme conditions (e.g., anaerobiosis, toxic metal salts); and the possibility of both intracellular and extracellular synthesis, which affords flexibility in downstream processing (Qamar and Ahmad, 2021).

Many bacterial species also possess innate resistance mechanisms to heavy metals, including the transformation of metal ions into less soluble or less toxic forms via intracellular accumulation or extracellular precipitation as nanoparticles (Beliaev and Saffarini, 1998). These capabilities have been harnessed to produce a variety of metallic nanoparticles, including silver

(AgNPs), gold (AuNPs), platinum (PtNPs), palladium (PdNPs), zinc oxide (ZnO NPs), copper oxide (CuO NPs), and selenium (Se NPs) (Iravani, 2014).

Bacterial synthesis may be intracellular—where NPs form inside the cell, often through enzyme-mediated reduction or metal sequestration in the cell envelope—or extracellular, where NPs form in the culture medium as a result of secreted redox-active metabolites (enzymes, flavins, proteins) (Hasan, 2015). Extracellular synthesis is generally preferred for industrial applications because it obviates biomass disruption for NP recovery, thereby reducing processing costs and facilitating purification (Eze and Nwabor, 2020).

The use of bacteria extends beyond nanoparticle formation to their functionalization: surface biomolecules (e.g., polysaccharides, glycoproteins) impart colloidal stability and can serve as platforms for targeted binding in biomedical applications (Dykman and Khlebtsov, 2012; Kora and Rastogi, 2015). Consequently, bacteria constitute a complex and versatile biosynthetic system that offers a unique combination of biological efficiency, sustainability, and process control for MNP synthesis, and they are central to advancing this "green nanotechnology" direction based on non-polluting methods.

Unlike conventional physico-chemical approaches, bacterial synthesis of MNPs proceeds under mild temperature and pH, requires no toxic solvents, and yields products that are naturally functionalized by cellular components. These advantages place bacterial biosynthesis at the forefront of current research into green nanotechnology.

1.9. Model bacteria used in MNP synthesis

Owing to their metabolic adaptability and capacity to interact with heavy metals, bacteria have been increasingly studied and employed as biological platforms for MNP synthesis. Their physiological and biochemical diversity enables both intracellular and extracellular routes, and their ability to reduce toxic metals to inert or functional forms confers a significant advantage over other biological systems (Narayanan and Sakthivel, 2010; Iravani, 2011).

Many bacterial species have been experimentally validated as efficient producers of MNPs (Iravani, 2014).

The genus Shewanella is particularly well studied for MNP synthesis due to extracellular electron transfer (EET) and the ability to reduce diverse metal ions, including Fe^{3+} , Mn^{4+} , U^{6+} , Ag^{+} , Au^{3+} , Pd^{2+} , and Pt^{4+} (Kotloski and Gralnick, 2013; Pirbadian et al., 2014; Egan-Morriss et al., 2022). Among the species, Shewanella oneidensis MR-1—Gram-negative, facultatively anaerobic, non-pathogenic, and metabolically versatile—is the preferred model (Rajput et al., 2021; Yu et al., 2022). Metal reduction is mediated by EET networks based on multihaem cytochromes located in the periplasm and outer membrane (MtrA/MtrB/MtrC, OmcA, CymA) and specialized porins (MtrB), which connect respiratory metabolism to extracellular metal acceptors (Beliaev et al., 2001; Beliaev and Saffarini, 1998; Maier and Myers, 2004; Shi et al., 2007, 2016; Coursolle and Gralnick, 2012; Fonseca et al., 2021; Paquette et al., 2023). Secreted flavins—riboflavin and FMN—act as redox mediators, initiating nucleation and stabilizing NPs, a role demonstrated electrochemically (von Canstein et al., 2008; Marsili et al., 2008; Kotloski and Gralnick, 2013). Production in spent medium facilitates purification and scalability (Khan et al., 2020; Boldt et al., 2023). NP localization varies with conditions and metal: extracellular; at the cell wall/periplasm; or intracellular (Shi et al., 2016; Kato et al., 2012; Ghosh et al., 2021; Chavez et al., 2025; Klaus et al., 1999).

1.10. Applications of nanoparticles synthesized by *S. oneidensis* across diverse fields

S. oneidensis MR-1 possesses a complex, finely tuned suite of metal-reduction mechanisms—including expanded respiratory chains, secretion of extracellular redox mediators, and structural adaptations of the membrane (Rajput et al., 2021). These features make it a key platform for sustainable, controlled, and reproducible MNP synthesis. A detailed understanding of these mechanisms provides a solid basis for leveraging this bacterium in industrial and biomedical applications of green nanotechnology.

AIMS AND OBJECTIVES OF THE THESIS

The aim of this thesis is to explore the redox potential of the bacterial strain S. oneidensis MR-1 for the production of noble-metal nanoparticles. The study focuses on three research directions: (1) obtaining MNPs using both bacterial cultures and the cell-free spent medium; (2) optimizing the redox properties of S. oneidensis MR-1 by inducing mutations in genes responsible for redox processes; and (3) assessing the antioxidant, antimicrobial, and dye-reducing potential of the resulting nanoparticles.

The general objectives were defined to reflect the complexity and interdisciplinary nature of the topic, as well as current challenges in existing protocols:

- To obtain MNPs (Au, Ag, Pt, Pd) using S. oneidensis MR-1 cell cultures and the cell-free spent medium generated during bacterial growth;
- To perform a comparative analysis of light versus darkness exposure in NP biosynthesis;
- To characterize the biosynthesized NPs using advanced techniques such as UV–Vis spectroscopy, transmission electron microscopy (TEM), and hyperspectral imaging (HSI);
- To obtain redox-enhanced mutant cells that could be used in future experiments;
- To evaluate the ecological applicability of the biosynthesized MNPs by reducing organic dyes;
- To test the antimicrobial and antioxidant activities of the biosynthesized MNPs as future directions for exploration in medicine.

By achieving these objectives, this work aims to contribute to the development of a robust and sustainable biotechnological framework capable of producing efficient, safe nanomaterials with a positive impact on the environment and human health.

PERSONAL CONTRIBUTIONS

CHAPTER II – MATERIALS AND METHODS

2.1. Bacterial strains used

Shewanella oneidensis MR-1 (LMG 19005), *Escherichia coli* WM3064, *Escherichia coli* ATCC 25922, and *Staphylococcus aureus* ATCC 6538.

2.2. Cultivation of bacterial strains

Shewanella oneidensis MR-1 (LMG 19005) was pre-cultured aerobically in 250 mL LB medium (Kim et al., 2017) containing yeast extract (5 g/L), sodium chloride (10 g/L), and tryptone (10 g/L).

E. coli WM3064 and *S. oneidensis* MR-1 used for generating mutants with enhanced redox properties were cultivated at 37 °C and 30 °C, respectively, in LB; for E. coli, the medium was supplemented with kanamycin (50 µg/mL). Cultures were incubated with shaking at 150 rpm.

For antibacterial testing, E. coli ATCC 25922 and *S. aureus* ATCC 6538 were grown in LB for 24 h at 37 °C with shaking at 200 rpm.

2.3. Biosynthesis of MNPs via anaerobic respiration

In the experiments performed, the terminal electron acceptors for anaerobic respiration were Pt, Pd, and Au ions. Bacterial biomass obtained in LB medium was washed with bicarbonate solution by centrifugation and resuspension, then incubated in buffer containing sodium lactate or sodium formate (as appropriate) together with the metal ions of interest, under anaerobic conditions, either in darkness or under illumination depending on the experiment.

2.4. Synthesis of AgNPs using the spent medium of S. oneidensis MR-1

Shewanella oneidensis cells were grown in LB for extended periods (up to 7 days). Cells were removed by centrifugation and filtration, $AgNO_3$ was added to the cell-free spent medium, and the mixture was incubated either under light or in the dark, as required.

2.5. UV–Vis spectrophotometry

PtNPs biosynthesis was monitored with a Specord 210 Plus spectrophotometer (Analytik Jena) over 220–800 nm, using UV–Vis cuvettes with a 1 cm optical path length.

2.6. Spectrofluorimetry

Fluorescence spectra of the synthesized Pt nanoparticles were recorded with an FP8300 spectrofluorometer (Jasco) using the following parameters: PMT 500 V, excitation wavelength 335 nm, and emission range (λ_em) 350–500 nm.

2.7. Transmission electron microscopy (TEM)

Shewanella oneidensis MR-1 cells bearing MNPs were fixed overnight at 4 °C in PBS with 2.5% glutaraldehyde, dehydrated through an ethanol series (10, 30, 50, 70, 90, and twice 100%; 15 min per step), and then examined by TEM. For determining the size and shape of extracted MNPs (as described in Section 2.7.1), samples were prepared for TEM by dispersing the particles in ultrapure (Milli-Q) water.

2.8. Dark-field microscopy and hyperspectral imaging (DF-HSI)

Cells were prepared as for TEM (fixed in 2.5% glutaraldehyde and dehydrated through graded ethanol solutions) and examined using a 100× oil-immersion objective.

2.9. Statistical analysis of MNP size and shape

Particle size and shape were analyzed with ImageJ (https://imagej.net/ij/). The procedure involved: (i) digitizing NP outlines; (ii) calculating each particle's diameter as the arithmetic mean of length and width; and (iii) determining the shape factor (width/length, W/L), with values close to 1 indicating spherical particles and lower values suggesting elongated or irregular shapes.

2.10. Generation of S. oneidensis MR-1 mutants

To enhance the redox capacity of S. oneidensis MR-1, mutants were generated by introducing random mutations into genes encoding cytochromes involved in extracellular electron transfer (EET), namely mtrC, omcA, and cymA.

RESULTS

CHAPTER III – BIOSYNTHESIS OF METALLIC NANOPARTICLES WITH *Shewanella oneidensis* MR-1

3.1. Obtaining MNPs with S. oneidensis MR-1 via anaerobic respiration

3.1.1. Biosynthesis and characterization of PdNPs

The reduction of Pd(II) to Pd(0) by Shewanella oneidensis MR-1 is visually indicated by the color change of the cell suspension from pink to light brown at 24 h and to dark brown at 72 h, consistent with an acceleration of reduction over time; these observations were corroborated by UV–Vis and fluorimetric measurements. For reliable spectral analysis, NP extraction from the biomass is required, since intact cells distort the spectra. In UV–Vis, a 1 mM $PdCl_2$ solution shows a maximum at ~400 nm (Pd(II)), whereas the PdNPs suspension exhibits low overall absorbance and lacks the 400 nm peak, suggesting reduction of Pd(II) to Pd(0), in agreement with the literature (Sriramulu and Sumathi, 2018; Veisi et al., 2017).

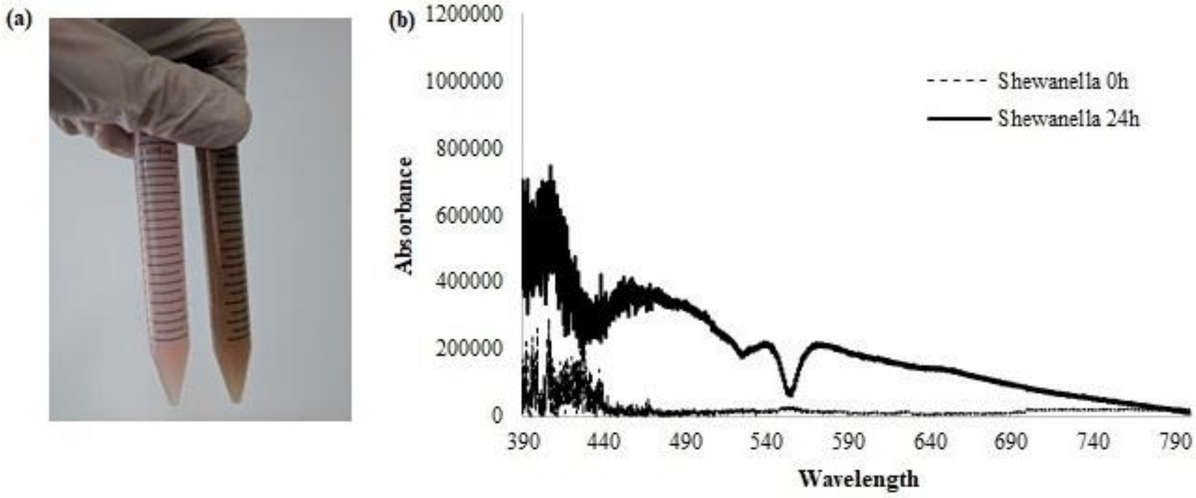

Figure 4. (a) Appearance of Shewanella oneidensis MR-1 cells grown anaerobically in the absence (left) and presence (right) of Pd(II). (b) UV–Vis spectra of S. oneidensis MR-1 cells grown anaerobically in the presence of Pd(II) at the initial time point (0 h) and after 24 h.

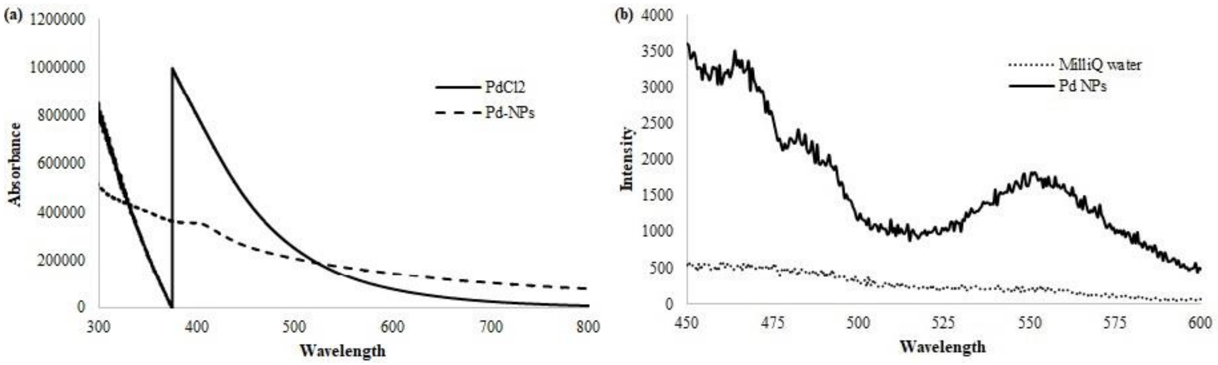

Figure 5. (a) UV–Vis spectra and (b) fluorescence spectra of an aqueous PdNPs solution extracted from Shewanella oneidensis MR-1, compared with the spectrum of $PdCl_2$ solution and that of deionized water, respectively.

The fluorimetric spectra of isolated PdNPs differ clearly from both the aqueous matrix and $PdCl_2$; at 260 nm excitation (500 V), $PdCl_2$ exhibits a narrow emission at ~521 nm, distinct in position and intensity from the PdNPs emission (Li et al., 2015; 2017). For comparison, chemically synthesized Pd nanoclusters show a maximum excitation wavelength around ~420 nm and an optimal emission near ~500 nm (Peng et al., 2018). Additional characterization (e.g., TEM) is required to correlate the emission profile with the size and shape of PdNPs produced by S. oneidensis MR-1.

Enhanced dark-field hyperspectral microscopy (HEDFM) highlights biosynthesized PdNPs predominantly on the exterior of S. oneidensis MR-1 cells and associated with the membrane, appearing as bright spots—supporting a role for extracellular and/or membrane-associated proteins in Pd(II) reduction (Ng et al., 2013). The observed localization agrees with the literature: NP <10 nm in the periplasm and NP ≥50 nm adhering to the outer membrane (de Windt et al., 2005; Dundas et al., 2018). Hyperspectral analysis on randomly selected cells shows clear differences: control cells have a maximum around ~600 nm, whereas PdNPs–bearing cells display a broader band with a maximum at 450–500 nm and a shoulder near ~600 nm, more pronounced in controls—changes consistent with PdNPs formation/attachment (Fig. 6a–c).

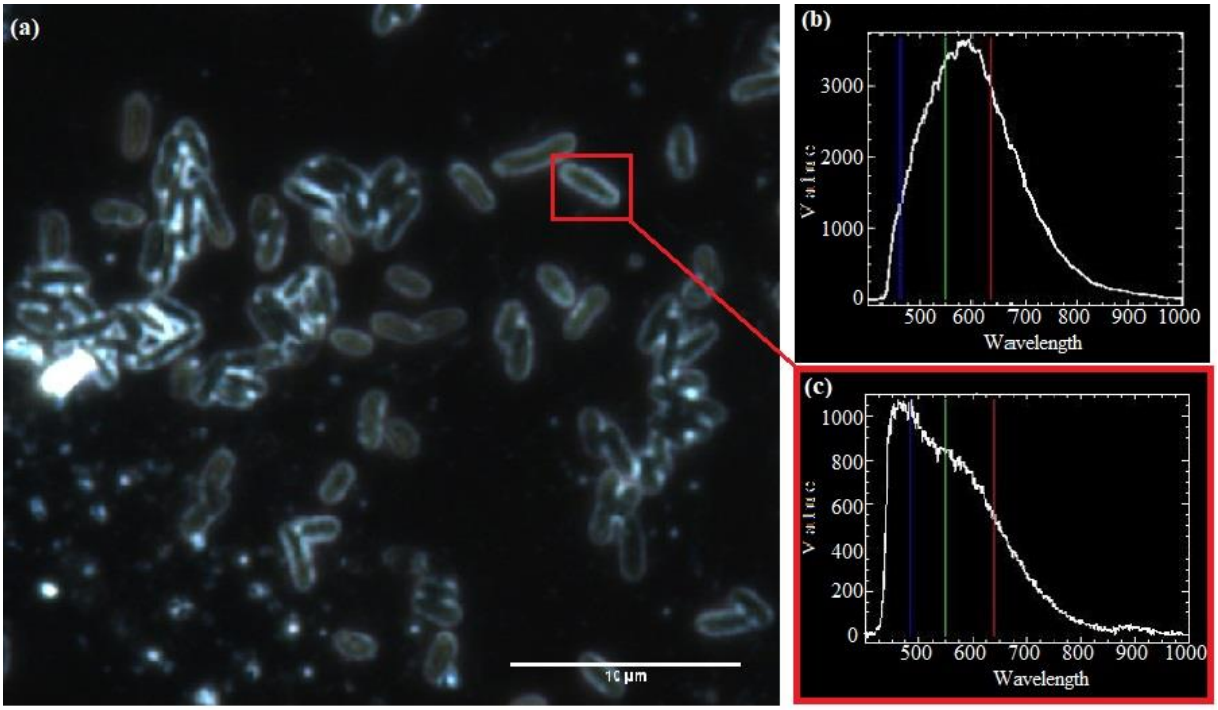

Figure 6. (a) Enhanced dark-field hyperspectral image of bacterial cells bearing PdNPs; (b) spectrum of control cells; and (c) spectrum of cells with PdNPs.

3.1.2. Biosynthesis and characterization of PtNPs

The PdNPs protocol was adapted to platinum(IV) using S. oneidensis MR-1. PtNPs formation was indicated visually by a color change of the suspension from pale yellow to black and, after centrifugation, of the biomass from pink to brown-black—a hue typical of Pt(0) (Fig. 7a). Process evolution was tracked by an increase in absorbance over 10 days (Fig. 7b); although bioreduction was slower than in some reports (likely due to trace O_2), the cells reduced and deposited PtNPs in the presence of formate as the electron donor. Control samples showed no color change, suggesting an absence of PtNPs synthesis.

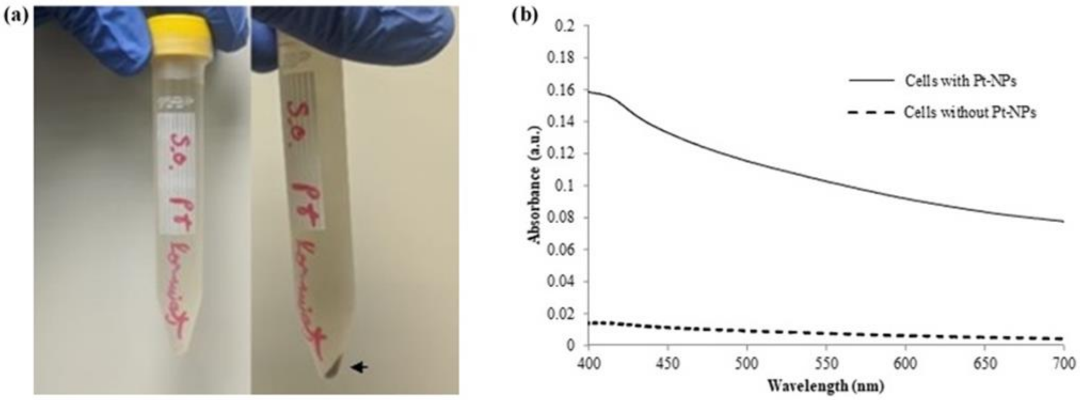

Figure 7. (a) S. oneidensis MR-1 in bicarbonate buffer with 1 mM H_2PtCl_6 at the start of the experiment (left) and after 10 days (right). (b) UV–Vis absorption spectra of cells with and without PtNPs in bicarbonate buffer after 10 days of incubation.

Reduction of Pt(IV)→Pt(0) was monitored by UV–Vis: the H_2PtCl_6 solution shows a maximum at ~260 nm (Pt(IV)), and the disappearance of this peak in the PtNPs suspension indicates Pt(0) formation (Nishanthi et al., 2019; Riddin et al., 2010; Charde et al., 2023) (Fig. 8a). Fluorimetrically, using an FP8300 (PMT 500 V, Ex 335 nm, emission range 350–500 nm), water exhibits a peak at ~380 nm, whereas PtNPs shows an intensified emission between 390 and 430 nm, with a maximum around ~430 nm (Fig. 8b). This behavior is consistent with the literature: Pt NPs typically display a weak plasmonic band in the UV (≈200–280 nm, as a shoulder), while ultrasmall particles (<2 nm) can emit strongly in the blue (≈400–480 nm), which explains the observed increase across 390–490 nm (Demishkevich et al., 2023; Wang et al., 2022; Chu et al., 2025).

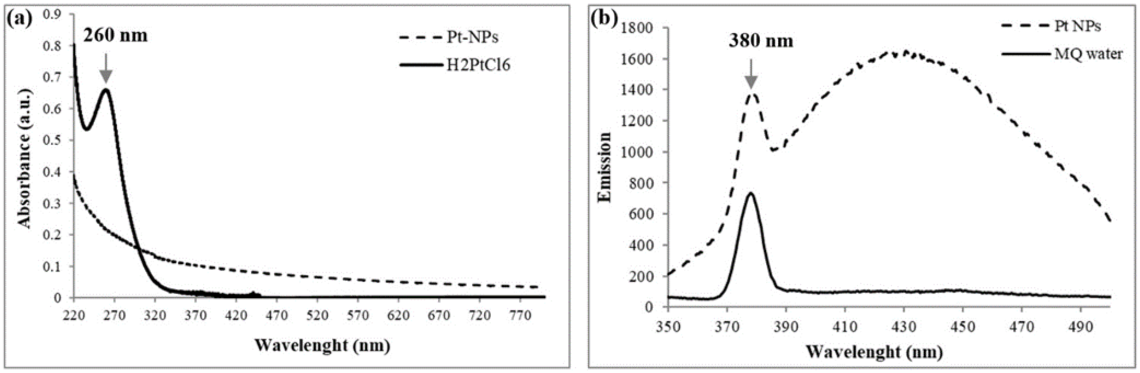

Figure 8. (a) UV–Vis spectrum of H_2PtCl_6 showing the characteristic maximum absorbance at 260 nm, and the absorption spectrum of extracted PtNPs. (b) Plasmonic emission of PtNPs.

Spectral analysis reveals clear differences between controls and platinized cells: the control shows a more pronounced peak around ~600 nm, whereas cells bearing PtNPs display a broadened band with a maximum at 600–700 nm and a shoulder at 500–600 nm (Fig. 9b–c). Together with UV–Vis/fluorimetry and TEM, these data confirm Pt(IV)→Pt(0) reduction in bicarbonate buffer with formate as the electron donor. For comprehensive structural and compositional validation, HR-TEM, SAED, EDS, and XRD are required.

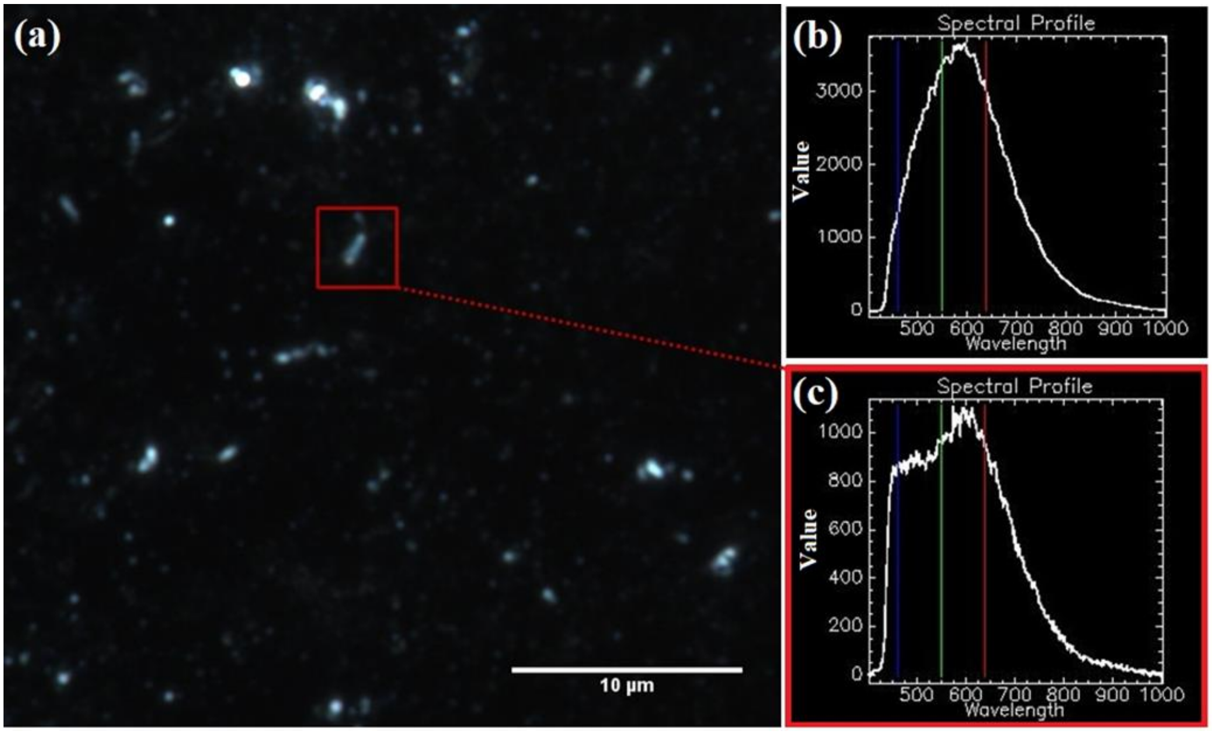

Figure 9. (a) Enhanced dark-field hyperspectral image of bacterial cells bearing PtNPs; (b) spectrum of control bacteria (no NPs); and (c) spectrum of a cell with PtNPs.

As shown in the TEM image in Fig. 10a, Shewanella oneidensis MR-1 is a cylindrical, rod-shaped bacterium measuring approximately 0.4 µm in width and 1.7 µm in length. Upon exposure to $H_2 PtCl_6$, the coloration shifted to black, attributable to the formation of PtNPs on the cell surface. To better resolve PtNPs size and shape, a fraction of the particles was extracted from the cells and visualized by TEM in bright-field and dark-field modes. Figures 10b and 10c show an ensemble of nearly spherical nanoparticles, 15–65 nm in size, with a mean diameter of ~36 nm (inset in Fig. 10a). Comparing the bright-field image in Fig. 10b with its dark-field counterpart in Fig. 10c, the NPs appear as much brighter, individually resolved spots—apparently monodisperse, discrete crystals—revealing the crystalline nature of the extracted PtNPs.

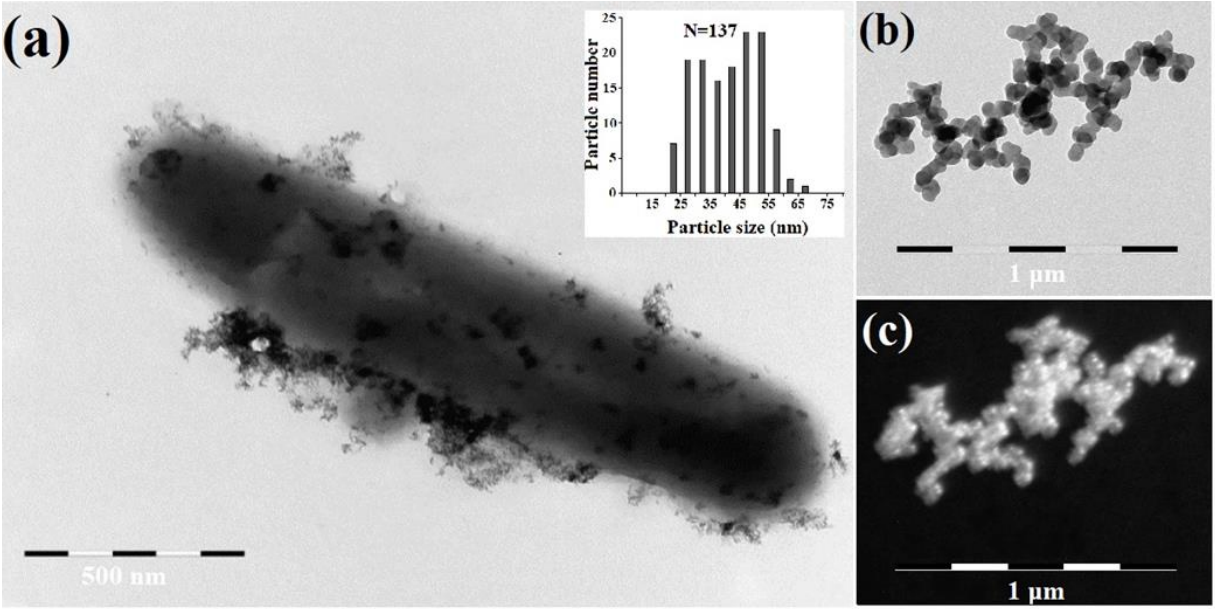

Figure 10. Visualization of PtNPs by TEM. (a) Bright-field TEM image of a *S. oneidensis* MR-1 cell after exposure to an aqueous 1 mM H_2PtCl_6 solution. PtNPs appear as electron-dense (dark) aggregates attached to the cell surface. Size distribution of the extracted PtNPs (inset). (b) Bright-field TEM image of PtNPs nanoparticles; (c) corresponding dark-field TEM image of biosynthesized PtNPs.

3.2. Effect of light on MNP synthesis

An important factor that can influence the activity of enzymes involved in metal-ion reduction is light (Huang et al., 2019). Exposure to white light (400–700 nm) accelerated and intensified the formation of Au, Pd, and Pt NPs compared with samples kept in the dark. After 24 hours under illumination, the gold samples turned pink, while the palladium- and platinum-containing samples began to blacken; in darkness, these changes appeared only after 48 hours. After six days, illuminated gold samples displayed a deep purple coloration and the Pd and Pt samples were completely black; in the dark, gold remained light pink, only one platinum sample turned black, and palladium blackened less intensely. These chromatic differences indicate more efficient metal reduction in the presence of light and confirm nanoparticle formation (Amendola et al., 2017; He et al., 2005).

Figure 11. Visual examination of color change after 144 h of incubation for: (a) Pt in the dark; (b) Pt under light; (c) Au under light; (d) Au in the dark; (e) Pd under light; (f) Pd in the dark; (g) Pt at the initial time point; (h) Au at the initial time point; (i) Pd at the initial time point.

UV–Vis measurements reveal clear differences between cell-containing samples and inorganic controls, confirming nanoparticle formation only in the presence of S. oneidensis MR-1. For palladium, the cell samples show a pronounced band at 390–400 nm, characteristic of PdNPs, with higher intensity under light (~740,000 a.u.) than in darkness (~680,000 a.u.), indicating more abundant particle formation upon illumination (Kalu et al., 2012; Ganesan and Ramasubbu, 2015; Koduru et al., 2017). For platinum, the characteristic H_2 $PtCl_6$ peak at ~260–265 nm is present at T0 but flattens in samples incubated under light, signaling Pt(IV)→Pt(0) reduction, whereas it remains partially in the dark, indicating incomplete reduction (Georgieva and Andonovsky, 2003). For gold, illuminated samples display a plasmonic maximum shifted to ~565 nm, consistent with the size/morphology dependence of the surface plasmon resonance, while no distinct band is observed in the dark—likely due to a lower concentration of Au NPs (He et al., 2005; Chen et al., 2008a; Amendola et al., 2017).

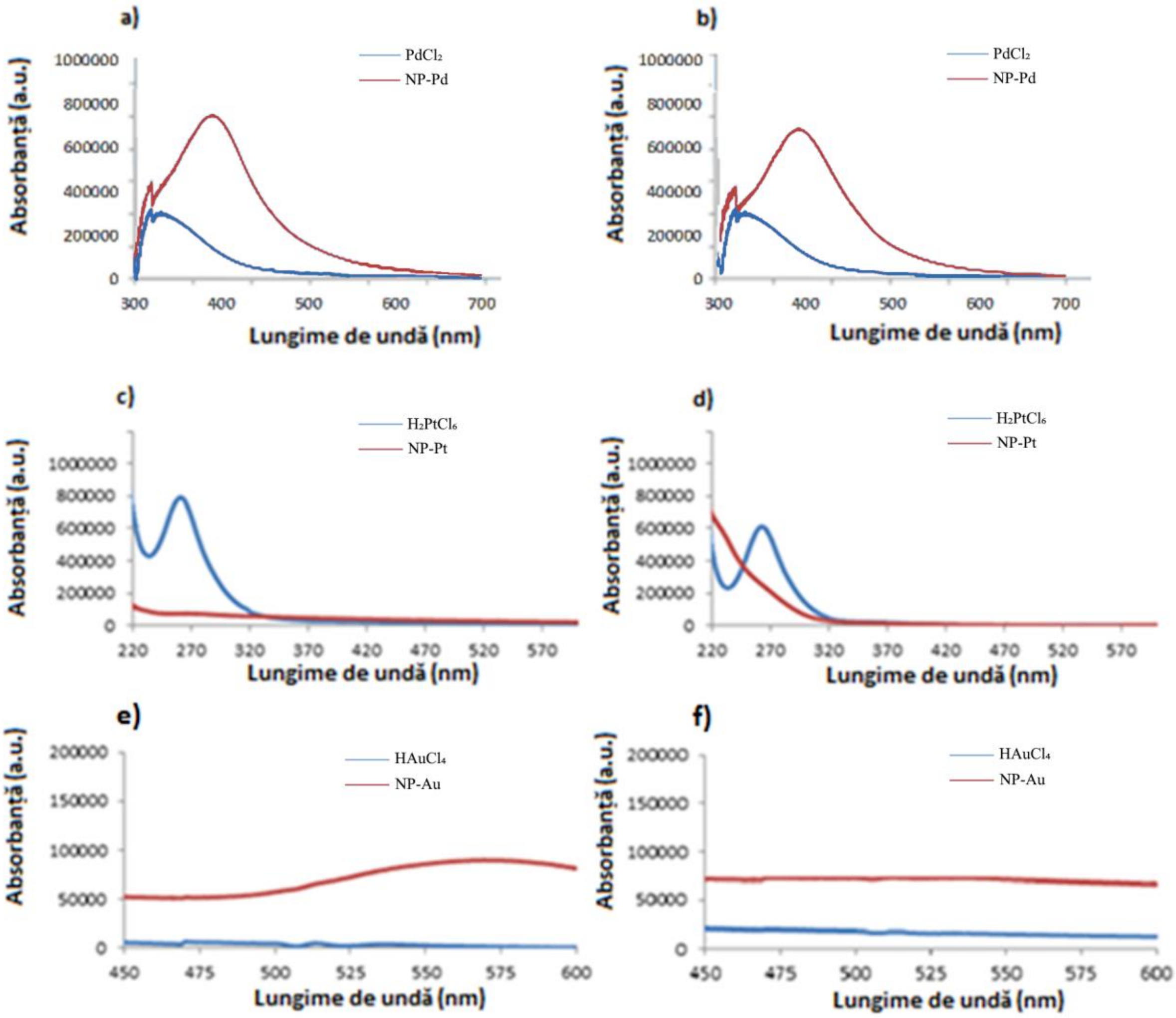

Figure 12. UV–Vis absorption spectra of (a) the Pd solution incubated under light and (b) in the dark; (c) the Pt solution under light and (d) in the dark; and (e) the Au solution under light and (f) in the dark, compared with the corresponding initial-time controls.

From Figure 13a–b it can be seen that, for Pt-treated cells under both light and dark conditions, the synthesized NPs are located on the outer and inner cell membranes as well as in the periplasmic space. Samples incubated with Pd under light (Fig. 13e) show a predominately membrane-associated distribution of NPs, similar to that observed for Pt and Au. By contrast, Pd NPs synthesized in the dark (Fig. 13f) display a different distribution, with fewer particles per unit area but a larger average size than those obtained under illumination. These light–dark differences may be attributable to the same mechanism implicated in the light-driven reduction of gold ions by S. oneidensis MR-1 described by Huang et al. (2019).

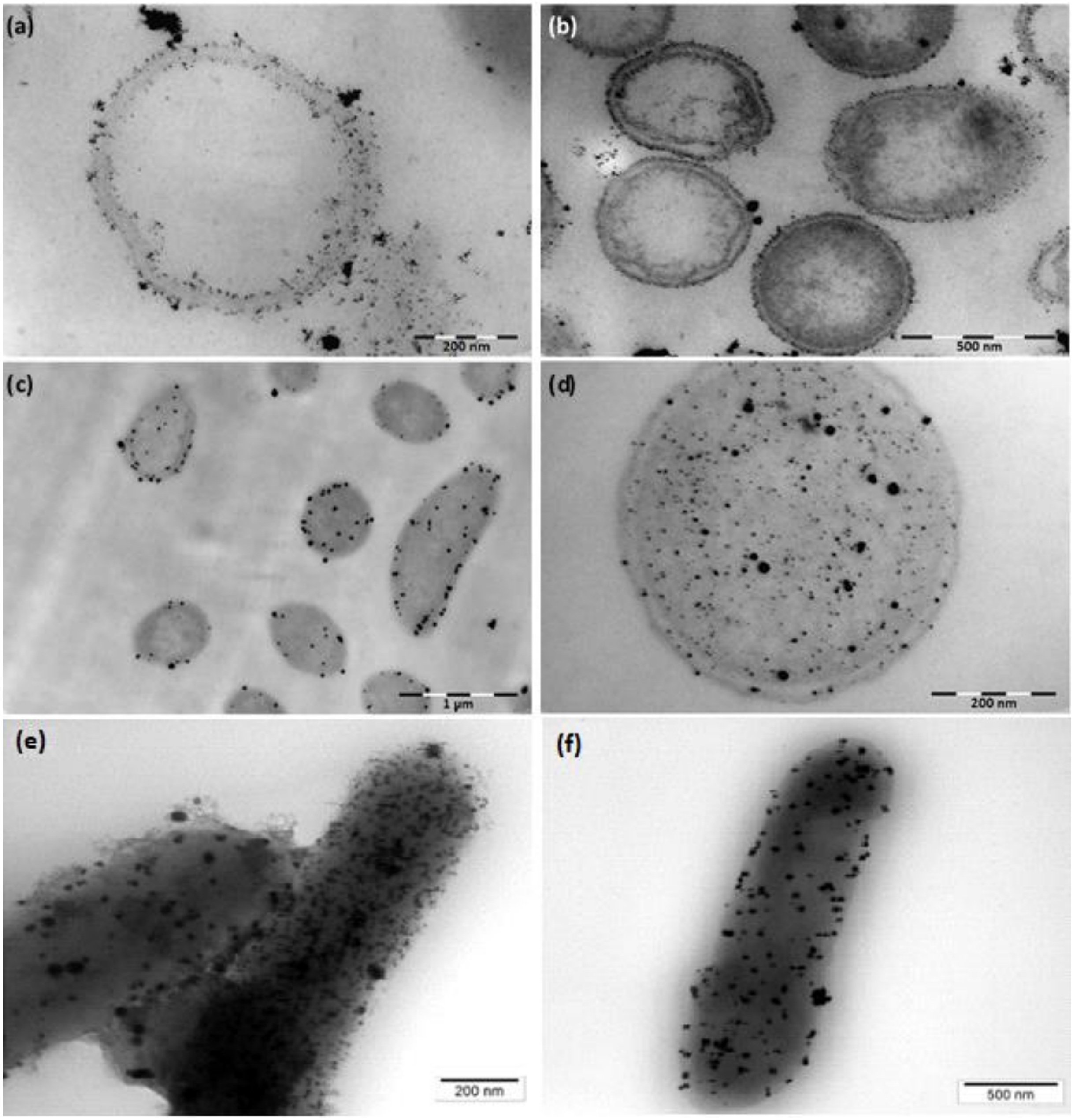

Figure 13. TEM images of Shewanella oneidensis MR-1 cells from samples: (a) Pt under light; (b) Pt in the dark; (c) Au under light; (d) Au in the dark.

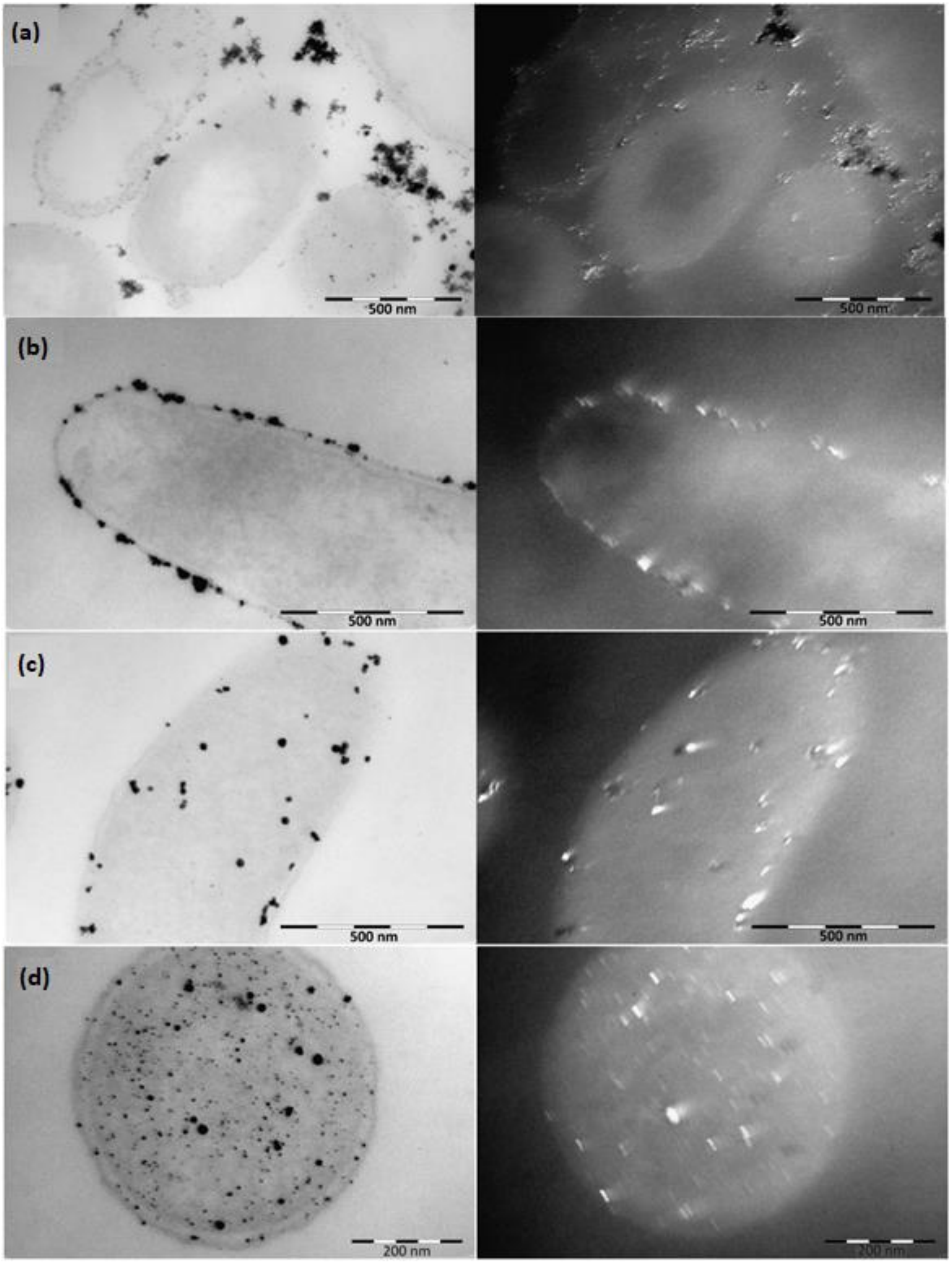

Figure 14. Bright-field TEM (left) and dark-field TEM (right) images of Shewanella oneidensis MR-1 cells from samples: (a) Pt under light; (b) Pt in the dark; (c) Au under light; (d) Au in the dark.

ImageJ measurements showed that the PtNPs obtained are very small, with a mean diameter of ~2 nm for particles synthesized under light (Fig. 15a) and ~1 nm for those synthesized in the dark (Fig. 15b), values comparable to sizes reported in the literature (e.g., ~5 nm) (Maes et al., 2017; Tuo et al., 2017; Xu et al., 2019). The spherical morphology of the PtNPs is likewise consistent with prior reports (Tuo et al., 2017).

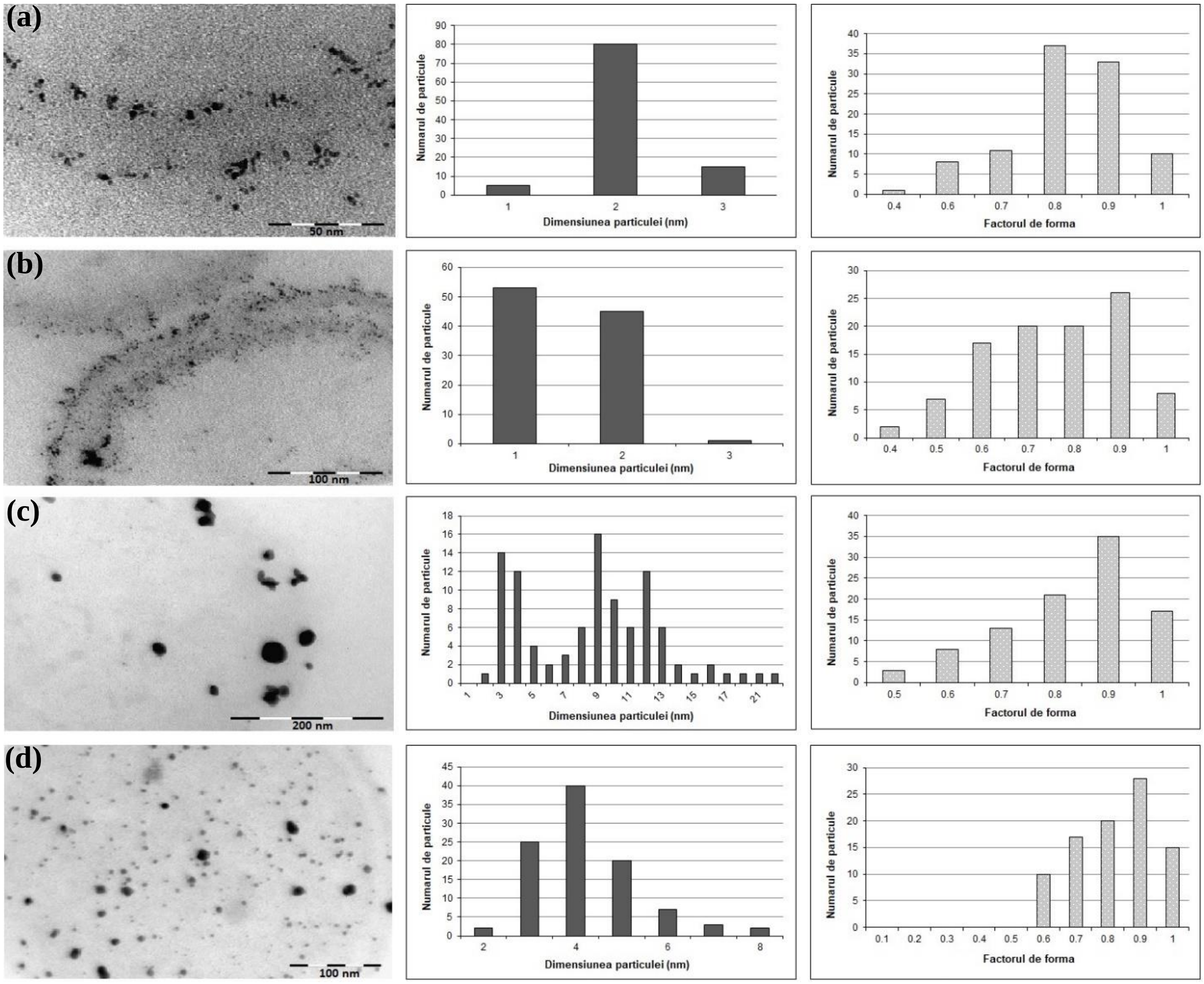

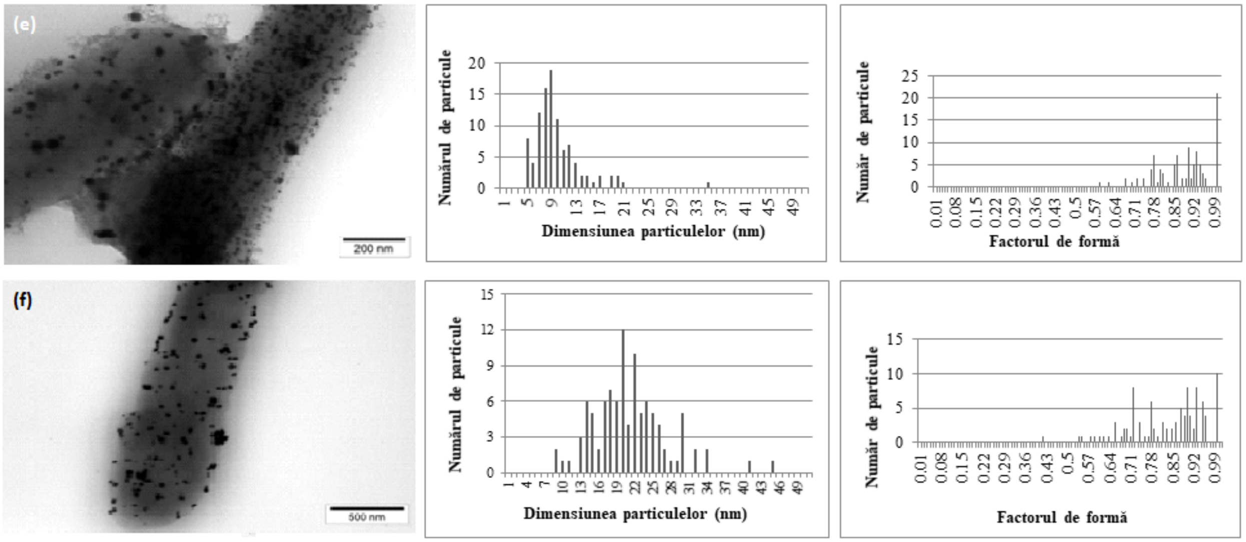

Figure 15. Size and shape distributions of PtNPs incubated (a) under light and (b) in the dark; AuNPs incubated (c) under light and (d) in the dark; and PdNPs incubated (e) under light and (f) in the dark, synthesized by S. oneidensis MR-1 cells.

3.3. Synthesis of AgNPs using the spent medium of *S. oneidensis* MR-1

The spent-medium approach harnesses the redox-active biomolecules secreted by S. oneidensis without the need to maintain bacterial viability, thereby simplifying the process and improving scalability. Recent studies have shown that spent media from bacterial and fungal cultures can efficiently mediate AgNP synthesis (Eze and Nwabor, 2020).

Consistent with prior reports indicating an increase in absorbance between 390 and 450 nm for silver nanoparticles (Kelly et al., 2003; Evanoff and Chumanov, 2005; Paramelle et al., 2014), UV–Vis analyses of the nanoparticles obtained in this study showed an increased absorbance in the 400–450 nm range, consistent with AgNP formation. These results are in agreement with bacterially mediated syntheses in which AgNPs produced in spent media display UV–Vis absorbance peaks around ~430 nm (Boldt et al., 2023).

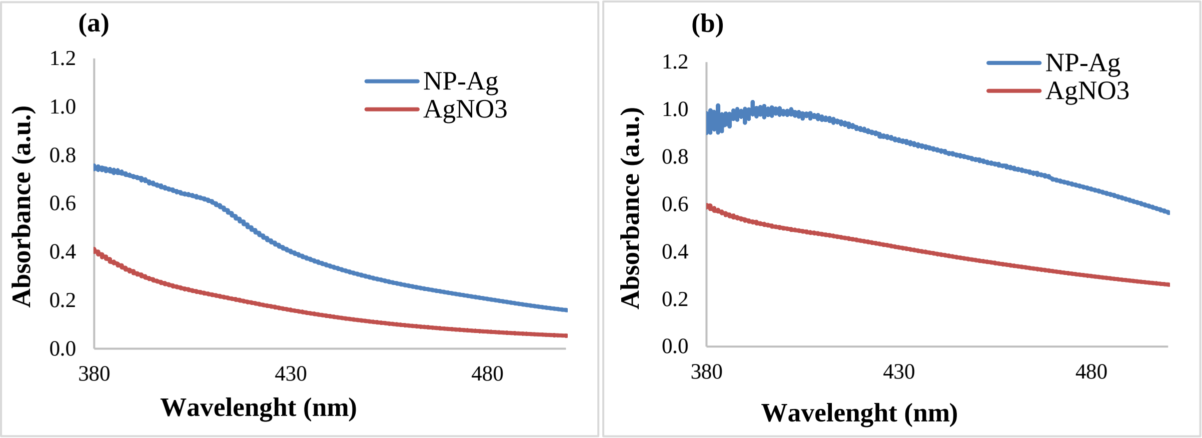

Figure 16. Absorption spectra of spent LB medium samples with AgNO$_3$ incubated (a) in the dark and (b) under light, compared with the initial-time control solutions.

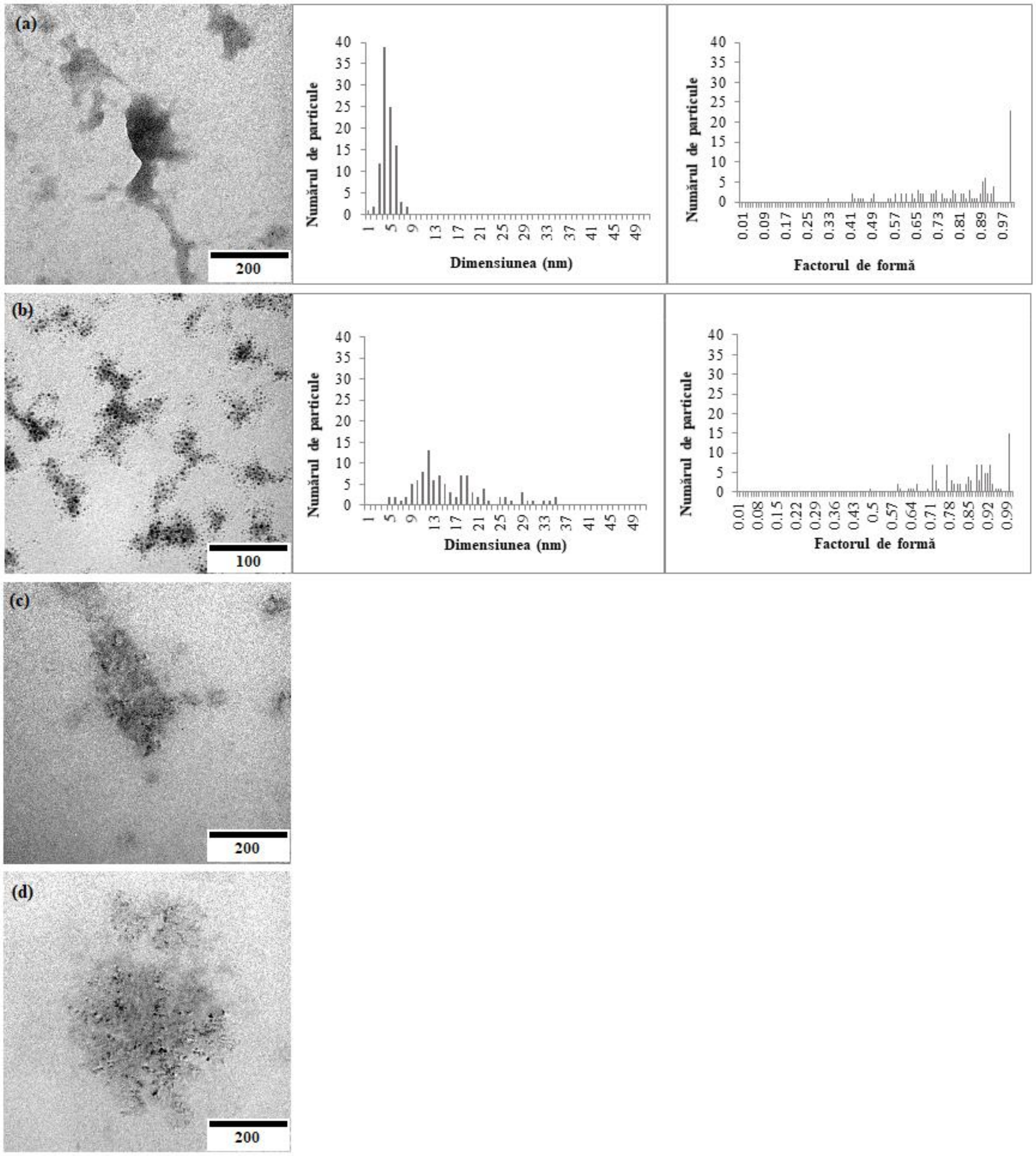

Figure 17. TEM images, size, and shape factor of AgNPs obtained with spent LB medium in the dark (a) and under light (b), and images of control samples ($AgNO_3$ in fresh LB medium) in the dark (c) and under light (d).

Confirmation of AgNP synthesis was obtained by TEM. TEM analysis revealed well-defined, spherical nanoparticles formed under both light and dark conditions (Fig. 17). However, significant differences were observed in the size distributions: AgNPs produced under illumination were markedly larger, with a mean diameter of 15.63 nm (Fig. 17), whereas those obtained in the dark were smaller, with a mean diameter of ~4 nm (Fig. 17).

CHAPTER IV – OBTAINING Shewanella oneidensis MR-1 MUTANTS TO ENHANCE THEIR REDOX CAPABILITIES

In this study, we aimed to generate mutants with improved redox capabilities. The pBBR1MCS plasmid was used to enable controlled expression of relevant genes, allowing comparison of redox capacity with that of S. oneidensis MR-1 (wild type) and the resulting mutants.

4.1. Induction of mutations in Shewanella oneidensis MR-1 cells

To optimize the redox activity of the S. oneidensis MR-1 strain, mutants were generated in three redox-related genes—*cymA*, *mtrC*, and *omcA*—using error-prone PCR.

The concentrations of the PCR products were as follows: *cymA*, 98.7 ng/µL; *mtrC*, 90.0 ng/µL; *omcA*, 72.6 ng/µL; and the pBBR vector, 62.4 ng/µL.

In an initial step, electrophoretic analysis (Fig. 18) revealed linearization of the pBBR plasmid digested with EcoRI and BamHI (~5,148 bp) and the absence of DNA fragments corresponding to *omcA*, *mtrC*, and *cymA*, indicating that cloning had not yet succeeded. After optimizing primer concentrations from 0.8 µM to 1.2 µM, the gene fragments *cymA* (~561 bp), *mtrC* (~1,723 bp), and *omcA* (~2,202 bp) were amplified, and NEBuilder assembly with linearized pBBR yielded the corresponding clones (Figs. 18–19). The recombinant DNA was purified for subsequent steps.

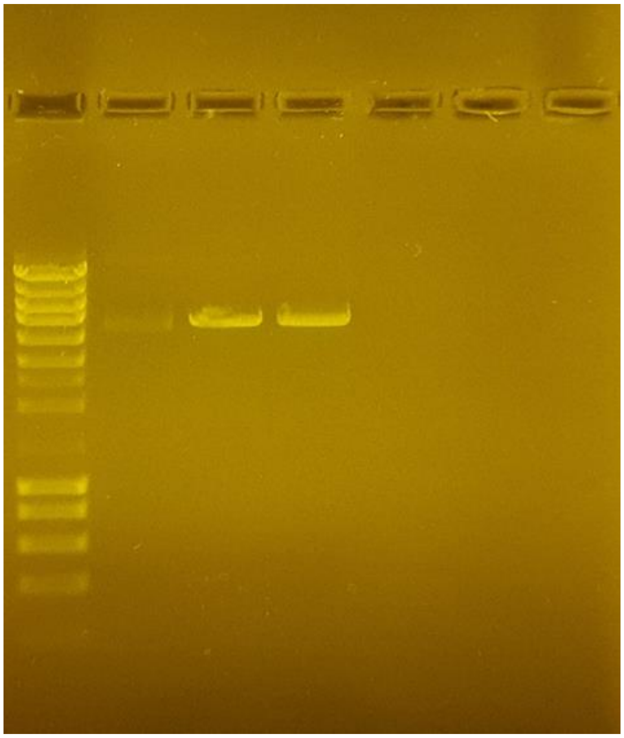

Figure 18. Agarose gel electrophoresis of the pBBR plasmid: undigested (lane 2), digested with EcoRI (lane 3) and BamHI (lane 4). PCR products for *cymA* (lane 5), *mtrC* (lane 6), and *omcA* (lane 7). Molecular weight marker: NZYTech (lane 1).

Following optimization of primer concentrations (from 0.8 µM to 1.2 µM), the gene fragments *cymA* (~561 bp), *mtrC* (~1,723 bp), and *omcA* (~2,202 bp) were successfully amplified (Myers and Myers, 1997; Beliaev et al., 2001; Johs et al., 2010), and double digestion of the resulting plasmids with EcoRI/BamHI confirmed recovery of the corresponding clones (Figs. 18–19).

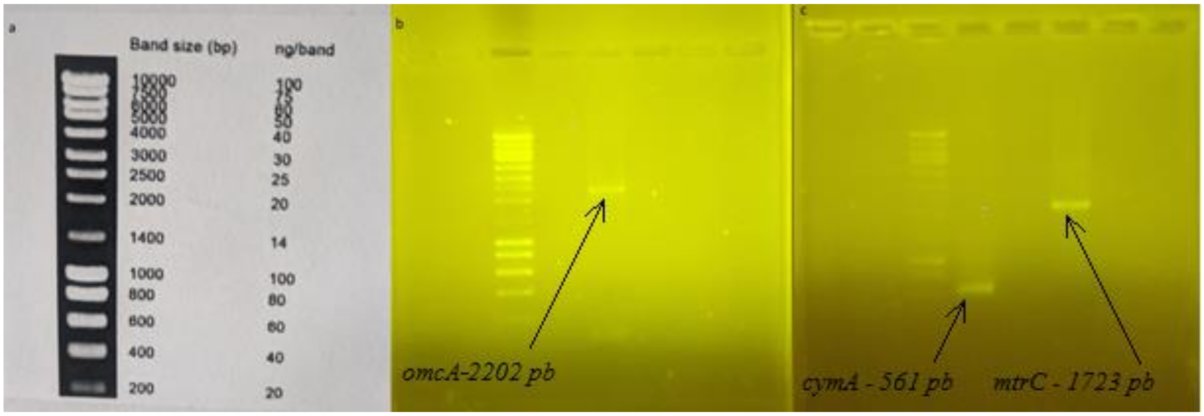

Figure 19. Electrophoretic analysis of DNA fragments obtained by error-prone PCR. (a) NZYTech molecular marker; (b) omcA gene (2,202 bp) — lane 5; (c) cymA gene (561 bp) —

lane 4 and mtrC gene (1,723 bp) — lane 6. The molecular weight marker appears in lane 3 in panels (b) and (c).

4.1.2. Expression of mutant cymA and omcA genes in Shewanella oneidensis MR-1

Expression was carried out at 30 °C in LB medium with kanamycin (50 µg/mL) for 24 h. Under these conditions, SDS–PAGE confirmed the presence of the recombinant CymA (~20.8 kDa) in the mutants and in the native strain. By contrast, OmcA (~85 kDa) was not detectable in the transformed strains, suggesting inefficient expression, possibly due to reduced mRNA stability or incorrect protein folding (Myers and Myers, 1997; Johs et al., 2010).

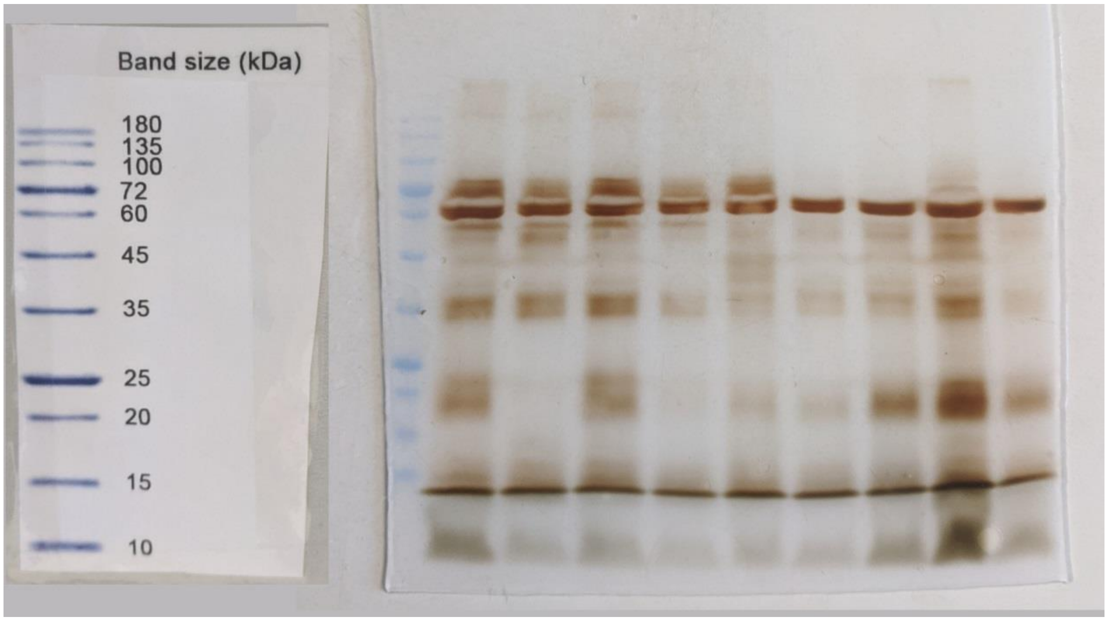

Figure 20. SDS–PAGE. Lane 1: molecular weight marker; 2: native CymA; 3: ΔCymA + pBBR (negative control); 4–5: CymA mutants #14 and #28; 6: native OmcA; 7: ΔOmcA ΔMtrC + pBBR (negative control); 8: OmcA mutant A.

4.2. Evaluation of the reducing potential of the obtained mutants

The cymA mutants exhibited enhanced redox activity compared with the native gene, particularly mutants 14, 16, and 28, which showed a faster dye-reduction rate (Fig. 21). In contrast, the omcA mutants displayed lower redox activity than the strain transformed with the native gene, indicating reduced extracellular electron transfer efficiency for these mutants (Fig. 22).

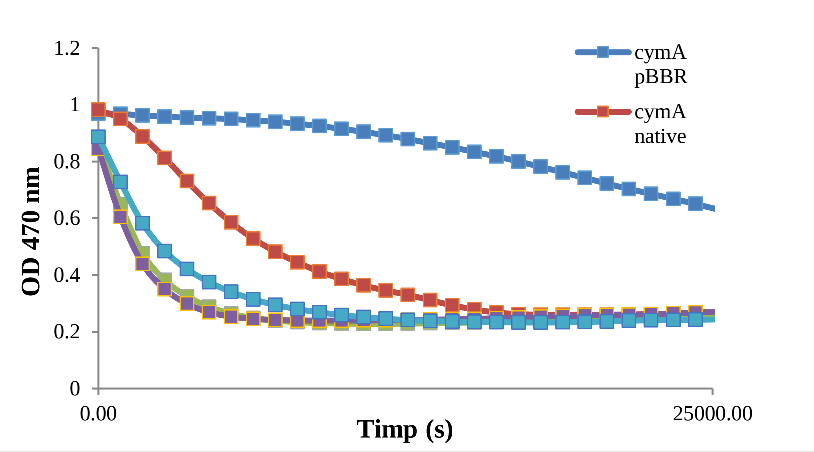

Figure 21. Redox activity of *S. oneidensis* CymA mutants (mutants 14, 16, 28). *S. oneidensis* strains transformed with the native *cymA* gene (*cymA* native), with the pBBR vector (*cym* pBBR), and with *cymA* mutants 14, 16, and 28.

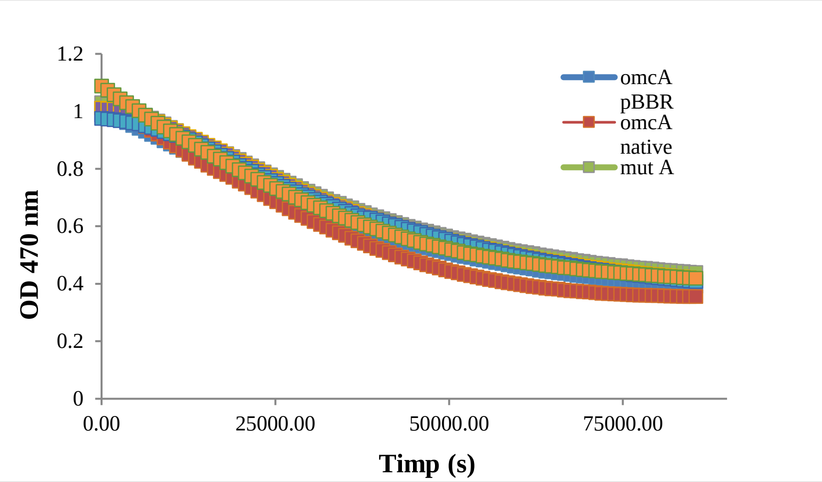

Figure 22. Redox activity of *S. oneidensis* OmcA mutants (mut A, B, C, I). *S. oneidensis* strains transformed with the native *omcA* gene (*omcA* native), with the pBBR vector (*omcA* pBBR), and with *omcA* mutants B, C, and I.

CHAPTER V – APPLICATIONS OF BIOSYNTHESIZED PLATINUM, PALLADIUM, GOLD, AND SILVER NANOPARTICLES

In these experiments, the potential applications of the experimentally obtained nanoparticles were investigated along three main directions: (i) catalytic degradation of two azo dyes—Congo red (CR) and methyl orange (MO)—and a cationic thiazine dye, methylene blue (MB); (ii) evaluation of antibacterial activity against *E. coli* and *S. aureus*; and (iii) determination of antioxidant capacity using the DPPH assay.

5.1. Dye reduction

The degradation of MB, CR, and MO was tested using PtNPs and AuNPs synthesized under light as well as in the dark. Reaction mixtures contained 4 µL nanoparticle suspension (1 mg/µL), 4 µL dye (1 mM), 6 µL sodium borohydride (100 mM), and 185 µL ultrapure (Milli-Q) water; the control lacked nanoparticles. For MB, PtNPs exhibited the best catalytic performance, with decolorization of 89.74% (PtNPs synthesized under light) and 87.18% (PtNPs obtained in the dark). In contrast, although AuNPs were less effective for MB, they outperformed for CR: samples treated with AuNPs—especially those produced in the dark—showed 82.11% decolorization, compared with only 18.42% for PtNPs obtained under light. For MO, all nanoparticle types yielded low decolorization percentages, ranging from 4.65% to 11.63%.

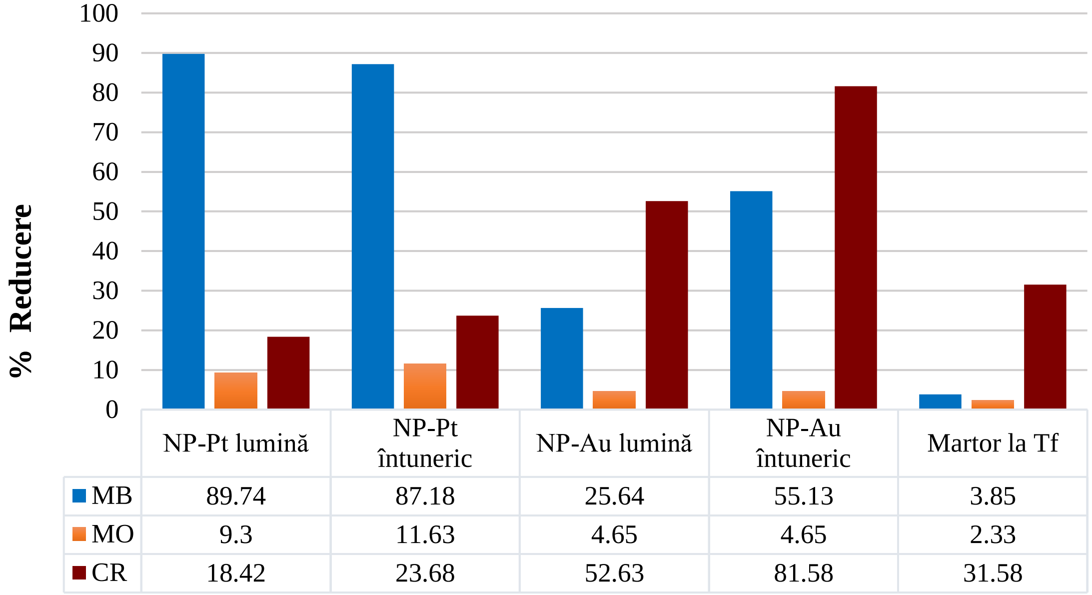

	NP-Pt lumină	NP-Pt întuneric	NP-Au lumină	NP-Au întuneric	Martor la Tf
🟦 MB	89.74	87.18	25.64	55.13	3.85
🟧 MO	9.3	11.63	4.65	4.65	2.33
🟥 CR	18.42	23.68	52.63	81.58	31.58

Figure 24. Percent reduction of MB ($\lambda = 662$ nm), MO ($\lambda = 465$ nm), and CR ($\lambda = 497$ nm) in the presence of: PtNPs synthesized under light, PtNPs synthesized in the dark, AuNPs synthesized under light, AuNPs synthesized in the dark, and the control solution at the final time point (Tf).

5.2. Antibacterial effect of MNPs

This study investigates the antibacterial activity of biogenically synthesized Ag, Au, Pd, and Pt NPs against the Gram-negative E. coli (ATCC 25922) and the Gram-positive S. aureus (ATCC 6538). Minimum inhibitory concentrations (MICs) were determined by the dilution method (Klančnik et al., 2010), while growth inhibition was evaluated via optical density measurements at 600 nm (OD_{600}) (Shamaila et al., 2016; Franzolin et al., 2022).

The results for S. aureus confirm the comparatively higher resistance of Gram-positive bacteria, yet clear differences emerged among the tested MNPs. Au NPs showed the most pronounced activity (100%, 67.2%, and 4.4%), and Pd NPs displayed a comparable profile—90.1% at the highest concentration and 54.6% at the medium dose, while still maintaining significant inhibition at the lowest dose (27.7%). Ag NPs exhibited a more limited effect on S.

aureus (99.8%, 23.5%, and 11.2%), whereas Pt NPs had the weakest antibacterial effect (64.1%, 17.5%, and 1%).

Table 6. Antibacterial effect of different biosynthesized MNP types—at low, medium, and high doses—against S. aureus and E. coli.

MNP	**% Inhibition *E.coli***			**% Inhibition *S. aureus***		
	Concentration			**Concentration**		
	Max 2 mg/L	**Mid 0,125 mg/L**	**Min0,008 mg/L**	**Max 2 mg/L**	**Mid 0,125 mg/L**	**Min 0,008 mg/L**
AgNPs	100	37,8	3,5	99,8	23,5	11,2
AuNPs	100	87	28,9	100	67,2	4,4
PdNPs	99,5	11,9	0,1	90,1	54,6	27,7
PtNPs	96,1	28,8	6	64,1	17,5	1

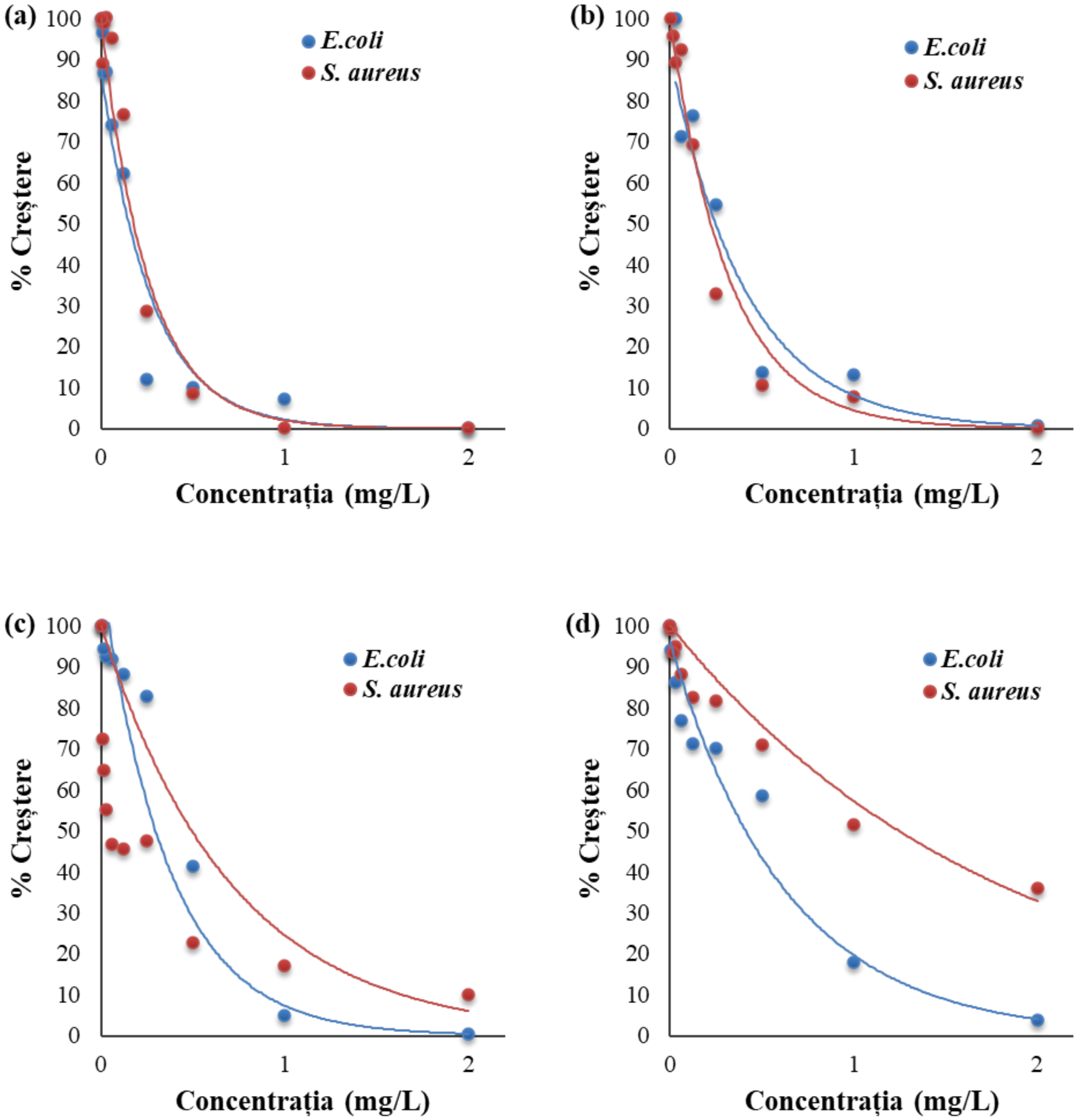

Figure 26. Effect of the concentration of different biosynthesized MNPs on bacterial growth: (a) AgNPs, (b) AuNPs, (c) PdNPs, (d) PtNPs. Values were corrected with the positive control (LB + inoculum + gentamicin) and normalized to the negative control (LB + inoculum, no NPs = 100% growth).

It can be observed that AgNPs and AuNPs display the strongest antibacterial potential, but with distinct activity profiles: AgNPs are more effective at higher concentrations, whereas

AuNPs maintain inhibitory effects even at lower doses. PdNPs show selective efficacy against Gram-positive bacteria, while PtNPs exhibit only limited activity.

5.3. Antioxidant effect of MNPs

The antioxidant activity of biosynthesized MNPs (Au, Ag, Pd, and Pt) was evaluated using the DPPH assay, a colorimetric method for determining free-radical scavenging capacity. The percentage of DPPH radical quenching was calculated relative to a negative control (DPPH solution without NPs) and a positive control (ascorbic acid) (Fig. 27).

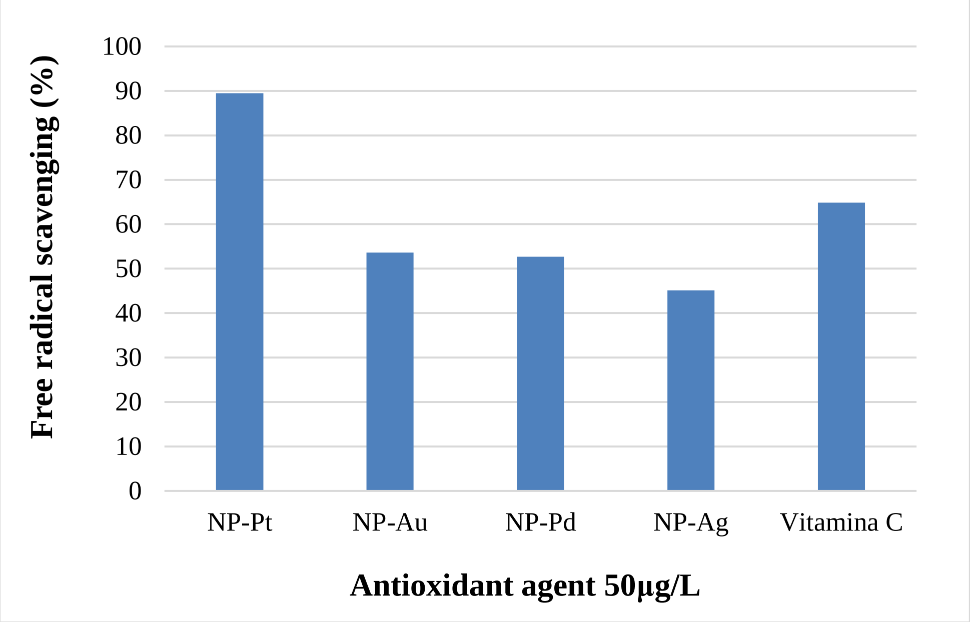

Figure 27. Antioxidant activity of different biosynthesized MNPs compared with vitamin C (positive control) and the negative control.

AuNPs and PdNPs exhibited intermediate antioxidant activity (53.63% and 52.72%, respectively). AgNPs showed the lowest activity among the MNPs analyzed (45.11%). Although ascorbic acid displayed higher antioxidant activity than most tested NPs, PtNPs proved an excellent alternative, with even greater efficiency (89.51%).

GENERAL CONCLUSIONS OF THE THESIS

This doctoral work leveraged the capacity of Shewanella oneidensis MR-1 to biosynthesize metallic nanoparticles (MNPs—Au, Ag, Pd, Pt) and examined their properties relevant to a broad range of applications. The experiments were designed around the versatility of the biological synthesis route used to obtain Au, Pt, Pd, and Ag NPs. For AgNPs, a spent-medium approach was employed, given the elevated toxicity of silver nitrate to bacteria; this strategy provides a simplified, cost-effective alternative and underscores the importance of selecting an appropriate biosynthesis environment, as also noted by Suresh et al., 2010.

The novelties of this work include: (i) the S. oneidensis MR-1–mediated production of NPs from multiple noble metals (Au, Pt, Pd, Ag), in a context where the literature on Pt and Pd NPs is comparatively limited; (ii) the generation of AgNPs using the spent medium of S. oneidensis MR-1 cultures; (iii) investigation of light effects on the Shewanella-mediated synthesis of Pd, Pt, and Ag NPs (a phenomenon previously documented predominantly for gold); and (iv) testing NPs obtained under both illumination and dark conditions, alongside exploring the impact of mutations in redox-related genes to enhance the bacterium's redox performance.

Studies on the influence of light showed that biosynthesis under illumination is more efficient than in darkness, in line with common reports in the literature. NPs obtained under light exhibited properties comparable to those produced in the dark; therefore, the photomediated route does not entail disadvantages in NP quality.

Genetic-engineering experiments highlighted the possibility of obtaining mutants with redox properties superior to the wild type, opening valuable prospects for biotechnological applications. Moreover, the importance of selecting the metal according to its intrinsic properties was evidenced by antibacterial and antioxidant assays, as well as by dye-reduction tests—findings with significance for medical and biotechnological fields and for ecology, including bioremediation.

Through spectroscopic and microscopic characterization, we carried out a detailed analysis of the produced nanoparticles, emphasizing the relationship between particle size and functional performance. Functional evaluations indicated that PtNPs deliver superior catalytic performance in methylene blue reduction, whereas AuNPs are more effective in degrading Congo red. Antioxidant and antibacterial activities of the synthesized NPs were also demonstrated: PtNPs proved even more effective than ascorbic acid in scavenging free radicals, and AgNPs showed the strongest antibacterial effect among all NPs tested against E. coli and S. aureus.

Overall, this research provides a multidisciplinary investigation of NP production using the S. oneidensis MR-1 platform and of process optimization toward potential applications of the resulting MNPs. Such an approach could support the development of automated MNP biosynthesis systems and their efficient deployment, opening avenues for impactful applications in medical, food, pharmaceutical, and environmental protection domains.

DISSEMINATION OF RESULTS

Articles published within the scope of the thesis

Papers published in ISI-indexed (Web of Science) journals:

1. Iacob, M.T., Ghinea, A., Morosanu, A.-M., Ardelean, I., Stamatin, S.N. & Moisescu, C. 2025 'Batteries to the rescue: the formation of Pt bioelectrocatalysts with Shewanella oneidensis MR-1 and commercial batteries', RSC Applied Interfaces, in press. (Equal contribution: Iacob and Ghinea.)

Papers published in journals indexed in international databases:

1. Iacob, M.T., Ghinea, A., Morosanu, A.-M., Ardelean, I., Stamatin, S.N. și Moisescu, C. 2025 'Batteries to the rescue: the formation of Pt bioelectrocatalysts with Shewanella oneidensis MR-1 and commercial batteries', RSC Applied Interfaces, in press. (Equal contribution: Iacob and Ghinea.)

Lucrări publicate în reviste indexate în baze de date internaționale:

1. **Ghinea, A.**, Moisescu, C., Iacob M.T., Morosanu A.M., & Ardelean I. 2021. *Bioreductive synthesis of platinum nanoparticles by Shewanella oneidensis MR-1*. Oltenia, Studii si Comunicari Seria Stiintele Naturii, 37(1): 192-198.
2. Moisescu, C., **Ghinea, A.**, Iacob, M.-T., Bălan, A., Stamatin, Ș. & Ardelean, I.I., 2019. *Palladium nanoparticle synthesis by Shewanella oneidensis MR-1*. Oltenia. Studii și Comunicări. Științele Naturii, 35(1): 183-188. ISSN 1454-6914.
3. Iacob, M.-T., **Ghinea, A**., Moisescu, C., Bălan, A., Stamatin, Ș. & Ardelean, I.I., 2019. *The evaluation of bacterial cultures redox potential in microbial fuel cells with different configurations*. Oltenia. Studii și Comunicări. Științele Naturii, 35(2): 156–160. ISSN 1454-6914.
4. **Ghinea, A.**, Moisescu, C., Moroșanu, A.-M. & Ardelean, I.I., 2022. *The influence of light on the biosynthesis of Pt and Au nanoparticles by Shewanella oneidensis MR-1*. Current Trends in Natural Sciences, 11(22), pp. 278–288. https://doi.org/10.47068/ctns.2022.v11i22.032
5. Brevet de invenție nr. RO 136027 B1, BOPI nr. 12 / 30.12.2024, cu titlul: Electrocatalizatori platinici obtinuți prin conversia bioelectrochimică a catalizatorilor auto uzați și procedeu de obținere a acestora. Autori: Stamatin Serban Nicolae, Moisescu

Cristina, Iacob Matei Tom, **Ghinea Adrian**, Diac Cornelia, Maxim Florentina Iuliana, Ardelean Ioan, Nichita Cornelia, Stamatin Ioan.

Short term scientific mission (STSM)

1. Ghinea, A. (2021). Short-Term Scientific Mission (STSM) – Scientific Report. COST Action CA19123 (PHOENIX). Host: ITQB NOVA, Lisbon, Portugal, September 19–October 2, 2021. e-COST ID: ECOST-STSM-Request-CA19123-48718. Document submitted to COST; available upon request.

Articles published in other fields

Book chapters

1. Moisescu, C., Ardelean, A.-V., Stamatin, Ș., **Ghinea, A.**, Iacob, M.-T., Voinea, S., Stamatin, I. & Ardelean, I.I., 2024. *Biological fuel cells with oxygenic photosynthetic microorganisms for wastewater treatment: State of the art and perspectives in bioanode*. In: N. Sahu & S. Sridhar, eds. *Algal biotechnology: Applications for industrial development and human welfare*. 1st ed. CRC Press, pp. 66–83 . DOI: 10.1201/9781003219194-6.
2. Stamatin, Ș., Iacob, M.-T., Moisescu, C., Ardelean, A.-V., **Ghinea, A**., Voinea, S., Stamatin, I. & Ardelean, I.I., 2024. *Biological fuel cells with oxygenic photosynthetic microorganisms for wastewater treatment: State of the art and perspectives in biocathode*. In: N. Sahu & S. Sridhar, eds. *Algal biotechnology: Sustainable energy solutions*. 1st ed. CRC Press, pp.101–110. DOI: 10.1201/9781003219156-10.

Conferences

1. **Ghinea, A**., Ardelean, I.I., Iacob, M.-T., Bălan, A., Stamatin, Ș. & Moisescu, C., 2020. *The bioreductive synthesis of platinum nanoparticles by Shewanella oneidensis MR-1*. The Scientific International Conference Museum and Scientific Research, 17 September 2020.
2. Iacob, M.-T., Ardelean, I.I., **Ghinea, A**., Moisescu, C., Bălan, A. & Stamatin, Ș., 2020. *Microbial fuel cells as devices for online monitoring of Shewanella oneidensis growth under aerobic conditions*. The Scientific International Conference Museum and Scientific Research, 17 September 2020.

SELECTED BIBLIOGRAPHY

1. Ahmad, A., Wei, Y., Syed, F., Tahir, K., Rehman, A.U., Khan, A.U., Ullah, S., Zaid, M., Raza, M. & Khan, F.U., 2016. Isatis tinctoria mediated synthesis of amphotericin B-bound silver nanoparticles with enhanced photoinduced antileishmanial activity. RSC Advances, 6(31), pp.25493–25503.
2. Alsaba, M.T., Al Dushaishi, M.F. & Abbas, A.K., 2020. A comprehensive review of nanoparticles applications in the oil and gas industry. Journal of Petroleum Exploration and Production Technology, 10, pp.1389–1399. Available at: https://doi.org/10.1007/s13202-019-00825-z.
3. Altammar KA. A review on nanoparticles: characteristics, synthesis, applications, and challenges. Front Microbiol. 2023 Apr 17;14:1155622. doi: 10.3389/fmicb.2023.1155622
4. Amendola, V. & Meneghetti, M. 2013. What controls the composition and the structure of nanomaterials generated by laser ablation in liquid solution? Physical Chemistry Chemical Physics, 15(9), 3027–3046. https://doi.org/10.1039/c2cp42895d
5. Amendola, V., Pilot, R., Frasconi, M., Maragò, O.M. & Iatì, M.A., 2017. Surface plasmon resonance in gold nanoparticles: a review. Journal of Physics: Condensed Matter, 29(20), p.203002. DOI: 10.1088/1361-648X/aa60f3.
6. Ardelean I.I. 2015. Metallic nanoparticle synthesis by cyanobacteria: fundamentals and applications. În: Sahoo D. Seckbach J. (eds) The Algae World. Cellular Origin, Life in Extreme Habitats and Astrobiology. 26, Springer, Dordrecht.
7. Arulmozhi, K.T. & Mythili, N., 2013. Studies on the chemical synthesis and characterization of lead oxide nanoparticles with different organic capping agents. AIP Advances, 3(12), p.122122. Available at: https://doi.org/10.1063/1.4858419.
8. Attard G., Casadesús M., Macaskie L.E., Deplanche K. 2012. Biosynthesis of platinum nanoparticles by Escherichia coli MC4100: can such nanoparticles exhibit intrinsic surface enantioselectivity? Langmuir. American Chemical Society Publisher. New York. 28: 5267-5274.
9. Baig, N., Kammakakam, I., Falath, W. 2021. Nanomaterials: a review of synthesis methods, properties, recent progress, and challenges. Materials Advances, 2(6), 1821–1871. https://doi.org/10.1039/D0MA00807A
10. Balachandran, A., Sreenilayam, S.P., Madanan, K., Thomas, S. & Brabazon, D., 2022. Nanoparticle production via laser ablation synthesis in solution method and printed electronic application – A brief review. Results in Engineering, 16, p.100646. Available at: https://doi.org/10.1016/j.rineng.2022.100646.
11. Batista C. A. S., Larson R. G., Kotov N. A. 2015. Nonadditivity of nanoparticle interactions. Science. 350(6257):1242477.
12. Beliaev, A. S., Saffarini, D. A., McLaughlin, J. L., Hunnicutt, D. 2001. MtrC, an outer membrane decahaem c cytochrome required for metal reduction in Shewanella putrefasciens MR-1. Molecular Microbiology, 39(3), 722–730. https://doi.org/10.1046/j.1365-2958.2001.02257.x

13. Beliaev, A. S., Saffarini, D. A., McLaughlin, J. L., Hunnicutt, D. 2001. MtrC, an outer membrane decahaem c cytochrome required for metal reduction in Shewanella putrefasciens MR-1. Molecular Microbiology, 39(3), 722–730. https://doi.org/10.1046/j.1365-2958.2001.02257.x
14. Boldt, A., Walter, J., Hofbauer, F., Stetter, K., Aubel, I., Bertau, M., Jäger, C.M. and Walther, T. 2023. Cell-free synthesis of silver nanoparticles in spent media of different Aspergillus species. Engineering in Life Sciences, 23(2), pp. 69–80. https://doi.org/10.1002/elsc.202200052
15. Buzea, C., Pacheco, I.I. & Robbie, K., 2007. Nanomaterials and nanoparticles: Sources and toxicity. Biointerphases, 2(4), pp.MR17–MR71. DOI: 10.1116/1.2815690.
16. Charde, R.P., van Devener, B. & Nigra, M.M. 2023. Surfactant- and ligand-free synthesis of platinum nanoparticles in aqueous solution for catalytic applications. Catalysts, 13(2), 246. doi:10.3390/catal13020246.
17. Chavez, M.S., MacLean, M.A., Sukenik, N., Yadav, S., Marks, C., El-Naggar, M.Y.. 2025. Synthesis of Palladium Nanoparticles by Electrode-Respiring Geobacter sulfurreducens Biofilms, ACS Biomaterials Science & Engineering, 11(1), 298–307. https://doi.org/10.1021/acsbiomaterials.4c01183
18. Chen H., Wei G., Ispas Adriana, Hickey S. G., Eychmuller A. 2010. Synthesis of palladium nanoparticles and their applications for surface-enhanced Raman scattering and electrocatalysis. The Journal of Physical Chemistry C. (50): 21976-21981.
19. Chen, H., Kou, X., Yang, Z., Ni, W. & Wang, J., 2008a. Shape- and size-dependent refractive index sensitivity of gold nanoparticles. Langmuir, 24(10), pp.5233–5237. DOI: 10.1021/la800305j. (a)
20. Chu, H.-W., Demissie, G.G., Huang, C.-C. & Anand, A. 2025. Protein-templated metal nanoclusters for chemical sensing. Frontiers in Analytical Science, 5:1510588.
21. Coursolle D., Gralnick J. A. 2012. Reconstruction of extracellular respiratory pathways for iron(III) reduction in Shewanella oneidensis strain MR-1. Frontiers in Microbiology, 3:56.
22. Daniel, M.-C. & Astruc, D., 2004. Gold nanoparticles: Assembly, supramolecular chemistry, quantum-size-related properties, and applications toward biology, catalysis, and nanotechnology. Chemical Reviews, 104(1), pp.293–346. DOI: 10.1021/cr030698+.
23. Das, D., Bhattacharyya, S., Bhattacharyya, M. & Mandal, P. 2022. Green chemistry inspired formation of bioactive stable colloidal nanosilver and its wide-spectrum functionalised properties for sustainable industrial escalation. Results in Chemistry, 4, 100533. https://doi.org/10.1016/j.rechem.2022.100533
24. De Windt W., Aelterman P, Verstraete W. 2005. Bioreductive deposition of Palladium (0) nanoparticles on Shewanella oneidensis with catalytic activity towards reductive dechlorination of polychlorinated biphenyls. Environ. Microbiol. 7(3): 314-25.
25. Dundas C. M., Graham A. J., Romanovicz D. K., Keitz B. K. 2018. Extracellular electron transfer by Shewanella oneidensis controls Pd nanoparticle phenotype. ACS Synthetic Biology. 7(12): 2726-2736.
26. Dykman, L.A. & Khlebtsov, N.G., 2012. Gold nanoparticles in biomedical applications: recent advances and perspectives. Chemical Society Reviews, 41(6), pp.2256–2282. DOI: 10.1039/C1CS15166E.

27. Egan-Morriss, C., Kimber, R.L., Powell, N.A., Lloyd, J.R. 2022. Biotechnological synthesis of Pd-based nanoparticle catalysts, Nanoscale Advances, 4(3), 690–705. https://doi.org/10.1039/D1NA00686J
28. El-Rafai, A.A., G. Ghoneim, D.A. & El-Rafai, N.A., 2018. Eco-friendly synthesis of metal nanoparticles using ginger and garlic extracts as biocompatible novel antioxidant and antimicrobial agents, 8(1), pp.71–81. DOI: 10.1007/s40097-018-0255-8.
29. Evanoff, D. D. Jr.; Chumanov, G. 2005. Synthesis and Optical Properties of Silver Nanoparticles and Arrays. ChemPhysChem, 6(7), 1221–1231.
30. Eze, F.N. & Nwabor, O.F., 2020. Valorization of Pichia Spent Medium via One-Pot Synthesis of Biocompatible Silver Nanoparticles with Potent Antioxidant, Antimicrobial, Tyrosinase Inhibitory and Reusable Catalytic Activities. Materials Science & Engineering C, 111, p.111104. DOI: 10.1016/j.msec.2020.111104.
31. Fonseca, B.M., Soares, R.M., Paquete, C.M. & Louro, R.O. 2021. Bacterial power: an alternative energy source. Enzymes for Solving Humankind's Problems, 215–246. doi:10.1007/978-3-030-58315-6_8.
32. Franzolin, M.R., Courrol, D.S., de Oliveira Silva, F.R. & Courrol, L.C., 2022. Antimicrobial activity of silver and gold nanoparticles prepared by photoreduction process with leaves and fruit extracts of Plinia cauliflora and Punica granatum.
33. Ganesan, V. & Ramasubbu, M. 2015. Environmental benign route in the synthesis of palladium nanoparticles using leaves of Acalypha indica L. International Journal of Pharma and Bio Sciences, 6, pp.603–610.
34. Georgieva, M., Andonovski, B. 2003. Determination of platinum(IV) by UV spectrophotometry. Analytical and Bioanalytical Chemistry, 375(6), 836–839. https://doi.org/10.1007/s00216-003-1783-7
35. Ghosh, S., Ahmad, R., Banerjee, K., AlAjmi, M.F., Rahman, S. 2021. Mechanistic aspects of microbe-mediated nanoparticle synthesis, Frontiers in Microbiology, 12, 638068. https://doi.org/10.3389/fmicb.2021.638068
36. Hachem, K., Ansari, M.J., Saleh, R.O., Kianfar, E., & Hammid, A.T., 2022. Methods of chemical synthesis in the synthesis of nanomaterial and nanoparticles by the chemical deposition method: A review. BioNanoScience, 12, pp.1032–1057. Disponibil la: https://doi.org/10.1007/s12668-022-00996-w.
37. Haefeli C., Franklin C., Hardy K. 1984. Plasmid-determined silver resistance in Pseudomonas stutzeri isolated from a silver mine. J. Bacteriol. 158(1): 389-392.
38. Haleem, A., Javaid, M., Singh, R.P., Rab, S. & Suman, R., 2023. Applications of nanotechnology in medical field: a brief review. Global Health Journal, [online] Available at: https://doi.org/10.1016/j.glohj.2023.02.008
39. Hasan, S., 2015. A Review on Nanoparticles: Their Synthesis and Types. Research Journal of Recent Sciences, 4(ISC-2014), pp.9–11. Disponibil la: https://www.isca.me/rjrs/archive/special-ISC-2014/3.ISCA-ISC-2014-Poster-3BS-63.pdf.
40. He S., Guo Z., Zhang Y., Zhang S., Wang J., GU N. 2007. Biosynthesis of gold nanoparticles using the bacteria Rhodopseudomonas capsulata. Materials Letters. Elsevier. London. 61(18): 3984-3987.

41. He, Y.Q., Tian, Z.Q., Shi, J.Y., Jiang, X.X., Huang, L.Q. & Yang, X.Y., 2005. A study on the sizes and concentrations of gold nanoparticles by spectra of absorption and scattering. Spectrochimica Acta Part A: Molecular and Biomolecular Spectroscopy, 61(13–14), pp.2861–2866. DOI: 10.1016/j.saa.2005.03.015.
42. Heim C. 2011. Microbial Biomineralization. In: Encyclopedia of Geobiology. Encyclopedia of Earth Sciences Series. Springer, Dordrecht. 586 pp.
43. Huang, B.C., Hu, C.W., Liao, C.H., Hsueh, Y.H. & Chen, Y.C., 2019. Photo-induction in Shewanella oneidensis MR-1 stimulates formation of Au NP. Scientific Reports, 9(1), p.7589. DOI: 10.1038/s41598-019-44023-2.
44. Husseiny M. I., El-Aziz M. A., Badr Y., Mahmoud M. A. 2007. Biosynthesis of gold nanoparticles using Pseudomonas aeruginosa. Spectrochim Acta A Mol Biomol Spectrosc. Elsevier. London. 67(3-4): 1003-1006.
45. Iravani, S., 2011. Green synthesis of metal nanoparticles using plants.
46. Iravani, S., 2014. Biosynthesis of nanoparticles: A green approach. Iranian Journal of Biotechnology, 12(2), pp.1–28. DOI: 10.5812/ijb.13591.
47. Jeevanandam, J., Barhoum, A., Chan, Y.S., Dufresne, A. & Danquah, M.K., 2018. Review on nanoparticles and nanostructured materials: history, sources, toxicity and regulations. Beilstein Journal of Nanotechnology, 9, pp.1050–1074. DOI: 10.3762/bjnano.9.98.
48. Johs A., Shi L., Droubay T., Ankner J. F., Liang L. 2010. Characterization of the decaheme c-type cytochrome OmcA in solution and on hematite surfaces by small angle x-ray scattering and neutron reflectometry. Biophysical journal, 98(12), 3035–3043. https://doi.org/10.1016/j.bpj.2010.03.049
49. Kalu, E., Daniel, M. & Bockstaller, M. 2012. Synthesis, characterization, electrocatalytic and catalytic activity of thermally generated polymer-stabilized metal nanoparticles. International Journal of Electrochemical Science, 7, pp.5297–5313. doi:10.1149/MA2010-01/13/779.
50. Kato, S., Hashimoto, K., Watanabe, K., 2012. Microbial interspecies electron transfer via electric currents through conductive minerals. Proceedings of the National Academy of Sciences, 109(25), pp.10042–10046.
51. Keat C. L., Aziz A., Eid A. M., Elmarzugi N. A. 2015. Biosynthesis of nanoparticles and silver nanoparticles. Bioresources and Bioprocessing. 2: 47.
52. Kelly, K. L.; Coronado, E.; Zhao, L. L.; Schatz, G. C. 2003. The Optical Properties of Metal Nanoparticles: The Influence of Size, Shape, and Dielectric Environment. Journal of Physical Chemistry B, 107(3), 668–677.
53. Khan, F.A., Zahoor, M., Khan, A., Ullah, R. & Wahab, A., 2017. A comprehensive review on synthesis, properties and applications of various types of nanoparticles. Journal of Nanomaterials, 2017, Article ID 8143853. DOI: 10.1155/2017/8143853.
54. Khan, M.R., Fromm, K.M., Rizvi, T.F., Giese, B., Ahamad, F., Turner, R.J., Füeg, M. & Marsili, E., 2020. Metal nanoparticle–microbe interactions: synthesis and antimicrobial effects. Physiological and Molecular Plant Pathology, Published online 17 March. https://doi.org/10.1002/ppsc.201900419

55. Klaus T, Joerger R, Olsson E, Granqvist CG (November 1999). "Silver-based crystalline nanoparticles, microbially fabricated". Proceedings of the National Academy of Sciences of the United States of America. 96 (24): 13611–13614. Bibcode:1999PNAS...9613611K. doi:10.1073/pnas.96.24.13611. PMC 24112. PMID 10570120
56. Koduru, M., Borelli, D.P.R., Park, S. & Kim, H. 2017. Synthesis and catalytic activity of alkylamine-capped ultra-small palladium nanoparticles for organic pollutant degradation. Journal of Cluster Science, 28, pp. 1–12. doi:10.1007/s10876-017-1262-5.
57. Kora, A.J. & Rastogi, L., 2015. Facile green synthesis of palladium nanoparticles using gum ghatti (Anogeissus latifolia): catalytic and biological applications. Journal of Environmental Chemical Engineering, 3(2), pp.1036–1043. DOI: 10.1016/j.jece.2015.03.016.
58. Kotloski, N. J., Gralnick, J. A. 2013. Flavin Electron Shuttles Dominate Extracellular Electron Transfer by Shewanella oneidensis. MBio, 4(1). https://doi.org/10.1128/mBio.00553-12
59. Lazăr V, Mărușescu L. G., Chifiriuc M. C.. 2017. Microbiologie Generală & Aplicată. Editura Universității din București.
60. Li H., Sun D. E., Liu Z. H. 2015. Ultrasensitive biosensing platform based on the luminescence quenching ability of plasmonic palladium nanoparticles. Chem. Eur. J. 21: 4944–4948.
61. Li H., Yang D., Li P., Zhang Q., Zhang W., Ding X., Mao J., Wu J. 2017. Palladium Nanoparticles-Based Fluorescence Resonance Energy Transfer Aptasensor for highly sensitive detection of Aflatoxin M_1 in milk. Toxins. 9(10): 318.
62. Li H., Yang D., Li P., Zhang Q., Zhang W., Ding X., Mao J., Wu J. 2017. Palladium Nanoparticles-Based Fluorescence Resonance Energy Transfer Aptasensor for highly sensitive detection of Aflatoxin M_1 in milk. Toxins. 9(10): 318.
63. Maes, S., Props, R., Fitts, J. P., de Smet, R., Vanhaecke, F., Boon, N., Hennebel, T. 2017. Biological recovery of platinum complexes from diluted aqueous streams by axenic cultures. PLoS ONE, 12(1), 1–17. https://doi.org/10.1371/journal.pone.0169093
64. Maier, T.M. & Myers, C.R., 2004. The outer membrane protein Omp35 affects the reduction of Fe(III), nitrate, and fumarate by Shewanella oneidensis MR-1. BMC Microbiology, 4, p.23.
65. Marsili, E., Baron, D. B., Shikhare, I. D., Coursolle, D., Gralnick, J. A., Bond, D. R. 2008. Shewanella secretes flavins that mediate extracellular electron transfer. Proceedings of the National Academy of Sciences, 105(10), 3968–3973. https://doi.org/10.1073/pnas.0710525105
66. McMillan, D.G.G., Marritt, S.J., Butt, J.N. & Jeuken, L.J.C. 2012. Menaquinone-7 is specific cofactor in tetraheme quinol dehydrogenase CymA. Journal of Biological Chemistry, 287(17), 14215–14225. https://doi.org/10.1074/jbc.M112.348813
67. Moisescu C., Ardelean I. I., Benning L. G. 2014. The effect and role of environmental conditions on magnetosome synthesis. Frontiers in Microbiology. 5: 49.

68. Myers Charles & Myers Judith. (1997). Cloning and sequence of cymA, a gene encoding a tetraheme cytochrome c required for reduction of iron(III), fumarate, and nitrate by Shewanella putrefaciens MR-1. Journal of bacteriology. 179. 1143-52. 10.1128/jb.179.4.1143-1152.1997.
69. Nangia Y., Wangoo N., Goyal N. Shekhawat G., Suri C. R. 2009. A novel bacterial isolate Stenotrophomonas maltophilia as living factory for synthesis of gold nanoparticles. Microb. Cell. Fact. BioMed Central Ltd. London. 8: 39.
70. Narayanan K. & Sakthivel N. 2010. Biological synthesis of metal nanoparticles by microbes. Advances in Colloid and Interface Science 156(1-2): 1-13.
71. Ng, C.K., Tan, T.K.C., Song, H., & Cao, B., 2013. Reductive formation of palladium nanoparticles by Shewanella oneidensis: role of outer membrane cytochromes and hydrogenases. RSC Advances, 5(70), pp.56433–56440.
72. Nishanthi R., Malathi S., Palani P. 2019. Green synthesis and characterization of bioinspired silver, gold and platinum nanoparticles and evaluation of their synergistic antibacterial activity after combining with different classes of antibiotics. Mater. Sci. Eng. C. Elsevier. London. 96: 693–707.
73. Paquete, C.M., Hapke, H., Martins, M.,2023. Elucidation of the electron transfer mechanisms of hydrogen production from light by Shewanella oneidensis - cadmium sulfide biohybrid system. Cell Reports Physical Science, 4(3), 100269.
74. Paramelle, D.; Sadovoy, A.; Gorelik, S.; Free, P.; Hobley, J.; Fernig, D. G. 2014. A Rapid Method to Estimate the Concentration of Citrate-Capped Silver Nanoparticles from UV-Visible Light Spectra. Analyst, 139, 4855–4861.
75. Peng Y., Wang P., Luo L., Liu L., Wang F. 2018. Green synthesis of fluorescent palladium nanoclusters. Materials. 11(2): 191.
76. Peng Y., Wang P., Luo L., Liu L., Wang F. 2018. Green synthesis of fluorescent palladium nanoclusters. Materials. 11(2): 191.
77. Pirbadian, S., Barchinger, S. E., Leung, K. M., Byun, H. S., Jangir, Y., Bouhenni, R. A., Reed, S. B., Romine, M. F., Saffarini, D. A., Shi, L., Gorby, Y. A., Golbeck, J. H., El-Naggar, M. Y. 2014. Shewanella oneidensis MR-1 nanowires are outer membrane and periplasmic extensions of the extracellular electron transport components. Proceedings of the National Academy of Sciences, 111(35), 12883–12888. https://doi.org/10.1073/pnas.1410551111
78. Potocnik J. Off J Eur Communities: Legis. 2011; L275:38–40. doi: 10.3000/19770677.L_2011.275.eng.
79. Qamar, S.U.R. & Ahmad, J.N., 2021. Nanoparticles: Mechanism of biosynthesis using plant extracts, bacteria, fungi, and their applications. Journal of Molecular Liquids, 337, p.116040. Available at: https://doi.org/10.1016/j.molliq.2021.116040.
80. Rafeeq, H., Hussain, A., Ambreen, A., Khan, A.A., Al-Zaqri, N. & Shkir, M., 2022. Functionalized nanoparticles and their environmental remediation potential: a review. Journal of Nanostructure in Chemistry, 12, pp.1007–1031. [online] Available at: https://doi.org/10.1007/s40097-021-00468-9.

81. Rajput, V.D., Minkina, T., Kimber, R.L., Singh, V.K., Shende, S., Behal, A., Sushkova, S., Mandzhieva, S. & Lloyd, J.R., 2021. Insights into the biosynthesis of nanoparticles by the genus Shewanella. Applied and Environmental Microbiology, 87(22), e01205-21. https://doi.org/10.1128/AEM.01205-21
82. Saif, S., Adil, S. F., Chaudhry, A., Khan, M. 2022. Microbial synthesis of magnetic nanomaterials. In Agri-Waste and Microbes for Production of Sustainable Nanomaterials (pp. 323–356). Elsevier. https://doi.org/10.1016/B978-0-12-823575-1.00020-2
83. Schmidt, H., 2001. Nanoparticles by chemical synthesis, processing to materials and innovative applications. Applied Organometallic Chemistry, 15(5), pp.331–343. Available at: https://doi.org/10.1002/aoc.169.
84. Shamaila, S., Zafar, N., Riaz, S., Sharif, R., Nazir, J. & Naseem, S., 2016. Gold nanoparticles: an efficient antimicrobial agent against enteric bacterial human pathogen. Nanomaterials, 6(4), p.71. DOI: 10.3390/nano6040071
85. Sharma, V. K., Yngard, R. A., & Lin, Y. 2012. Silver nanoparticles: Green synthesis and their antimicrobial activities. Advances in Colloid and Interface Science, 145(1–2), 83–96. https://doi.org/10.1016/j.cis.2008.09.002
86. Shi, L., Dong, H., Reguera, G., Beyenal, H., Lu, A., Liu, J., Yu, H-Q. & Fredrickson, J.K. 2016. Extracellular electron transfer mechanisms between microorganisms and minerals. Nature Reviews Microbiology, 14, 651–662. https://doi.org/10.1038/nrmicro.2016.93
87. Shi, L., Squier, T.C., Zachara, J.M. & Fredrickson, J.K. 2007. Respiration of metal (hydr)oxides by Shewanella and Geobacter: a key role for multiheme c-type cytochromes. Molecular Microbiology, 65(1), 12–20. https://doi.org/10.1111/j.1365-2958.2007.05783.x
88. Siddiqi K. S. & Husen A. 2016. Green synthesis, characterization and uses of Palladium/Platinum nanoparticles. Nanoscale Research Letters. 11: 482.
89. Singh, Y., Javier, J.R.N., Ehrman, S.H., & Magnusson, M.H., 2002. Approaches to increasing yield in evaporation/condensation nanoparticle generation. Journal of Aerosol Science, 33(9), pp.1309–1325. Available at: https://doi.org/10.1016/S0021-8502(02)00072-1.
90. Sriramulu M. & Sumathi S. 2018. Biosynthesis of palladium nanoparticles using Saccharomyces cerevisiae extract and its photocatalytic degradation behaviour. Adv. Nat. Sci.: Nanosci. Nanotechnol. 9(2): 025018-025024.
91. Suresh A. K., Doktycz M. J, Wang W., Moon J., Gu B., Meyer 3rd H. M, Hensley D. K., Allison D. P., Phelps T. J., Pelletier D. A. 2011. Monodispersed biocompatible silver sulfide nanoparticles: Facile extracellular biosynthesis using the γ -proteobacterium, Shewanella oneidensis. Acta Biomaterialia. 7(12): 4253-4258.
92. Thanh, N.T.K., Maclean, N. & Mahiddine, S., 2014. Mechanisms of nucleation and growth of nanoparticles in solution. Chemical Reviews, 114(15), pp.7610–7630.
93. Thatoi, P., Kerry, R.G., Gouda, S., Das, G., Pramanik, K., Thatoi, H. & Patra, J.K., 2016. Photo-mediated green synthesis of silver and zinc oxide nanoparticles using aqueous extracts of two mangrove plant

species, Heritiera fomes and Sonneratia apetala, and investigation of their biomedical applications. Journal of Photochemistry and Photobiology B: Biology, 163, pp.311–318.

94. Tuo, Y., Liu, G., Dong, B., Yu, H., Zhou, J., Wang, J., Jin, R. 2017. Microbial synthesis of bimetallic PdPt nanoparticles for catalytic reduction of 4-nitrophenol. Environmental Science and Pollution Research, 24(6), 5249–5258. https://doi.org/10.1007/s11356-016-8276-7
95. Veisi H., Hemmati S., Qomi M. 2017. Aerobic oxidation of benzyl alcohols through biosynthesized palladium nanoparticles mediated by Oak fruit bark extract as an efficient heterogeneous nanocatalyst. Tetrahedron Letters. 58(44): 4191-4196.
96. von Canstein, H., Ogawa, J., Shimizu, S., Lloyd, J.R., 2008. Secretion of flavins by Shewanella species and their role in extracellular electron transfer. Applied and Environmental Microbiology, 74(3), pp.615–623.https://doi.org/10.1128/AEM.01387-07
97. Wang W, Nadagouda MN, Mukhopadhyay SM. 2022. Advances in Matrix-Supported Palladium Nanocatalysts for Water Treatment. Nanomaterials (Basel). Oct 13;12(20):3593. doi: 10.3390/nano12203593. PMID: 36296782; PMCID: PMC9612339.
98. Xu, H., Xiao, Y., Xu, M., Cui, H., Tan, L., Feng, N., Liu, X., Qiu, G., Dong, H., Xie, J. 2019. Microbial synthesis of Pd–Pt alloy nanoparticles using Shewanella oneidensis MR-1 with enhanced catalytic activity for nitrophenol and azo dyes reduction. Nanotechnology, 30(6), 065607. https://doi.org/10.1088/1361-6528/aaf2a6
99. Yates M. D., Cusick R. D., Logan B. E. 2013. Extracellular palladium nanoparticle production using Geobacter sulfurreducens. ACS Sustainable Chemistry & Engineering. American Chemical Society Publisher. New York. 1(9): 1165-1171.
100. Yu, K., Huang, Z., Xiao, Y. & Wang, D., 2022. Shewanella infection in humans: epidemiology, clinical features and pathogenicity. Virulence, 13(1), pp.1515–1532. Available at: https://doi.org/10.1080/21505594.2022.2117831.
101. Zayadi, R. A., & Bakar, M. F. A. 2020. Biosynthesis of gold nanoparticles using Spirulina platensis and Chlorella vulgaris extracts and evaluation of their antioxidant activities. Journal of King Saud University - Science, 32(1), 1116–1122. https://doi.org/10.1016/j.jksus.2019.09.004
102. Zou, L., Zhu, F., Long, Z., Huang, Y. 2021. Bacterial extracellular electron transfer: a powerful route to the green biosynthesis of inorganic nanomaterials for multifunctional applications. Journal of Nanobiotechnology, 19(1), 120. https://doi.org/10.1186/s12951-021-00868-7